DOI: 10.1039/D1PY00694K (Review Article) *Polym. Chem.*, 2021, **12**, 4130-4158

Recent developments towards performance-enhancing lignin-based polymers

Garrett F. Bass† [a] **and Thomas H. Epps† III** *[abc]

[a]*Department of Chemical and Biomolecular Engineering, University of Delaware, Newark, Delaware 19716, USA. E-mail: thepps@udel.edu*

[b]*Department of Materials Science and Engineering, University of Delaware, Newark, Delaware 19716, USA*

[c]*Center for Research in Soft matter and Polymers (CRiSP), University of Delaware, Newark, Delaware 19716, USA*

Received 24th May 2021 , Accepted 5th July 2021

First published on 6th July 2021

Abstract

Fossil fuels are a cheap and abundant feedstock for polymeric materials that have enabled innumerable quality-of-life improvements. Yet, their declining supply and non-renewable nature have driven the pursuit of bio-based alternatives. Lignin represents the largest natural source of aromatic carbon on the planet, and thus, lignin-derived products have emerged as critical elements in the next generation of polymers. The relative abundance, large concentration of functional handles, and thermal stability of lignin make it an attractive target for bio-based polymers. However, the valorization of lignin to high-performance and cost-competitive materials remains a challenge. In this review, developments in the translation of lignin into value-added macromolecular components are discussed. Strategies to incorporate bulk lignin in polymer blends

and composites are introduced with a focus on applications. Furthermore, recent advances in the preparation of higher-value thermoplastics, thermosets, and vitrimers from deconstructed lignin products are highlighted from a synthetic perspective. Finally, key hurdles and future opportunities in lignin valorization are explored.

Garrett F. Bass

Garrett Bass received a B.S. in Biochemistry from the California Polytechnic State University, San Luis Obispo while also conducting research under Prof. Philip J. Costanzo. He completed his Ph.D. in 2020 at the University of Akron under the supervision of Prof. Matthew L. Becker. His work primarily focused on developing novel stereolithographic printing strategies for biomedical devices. In 2020, he started a postdoctoral position under Prof. Thomas H. Epps, III at the University of Delaware (UD), where he works on the synthesis and characterization of lignin-inspired polymers.

Thomas H. Epps, III

Thomas H. Epps, III is the Allan & Myra Ferguson Distinguished Professor of Chemical & Biomolecular Engineering at UD. He holds a joint appointment in Materials Science & Engineering and is the Director of the Center for Research in Soft matter & Polymers (CRiSP) and Center for Hybrid, Active, and Responsive Materials (CHARM). He is also Deputy Director of the Center for Plastics Innovation (CPI). Prof. Epps earned his B.S. (1998) and M.S. (1999) in Chemical Engineering from MIT. He completed his Ph.D. in Chemical Engineering at the University of Minnesota (2004) and was a Postdoctoral Fellow at NIST (2004–2006). His research interests include renewable chemicals and polymers from biomass and polymer waste streams, ion-conducting nanostructured materials, polymer thin films, self-assembling polymers for nucleic acid delivery, and polymer composites. Prof. Epps is also a cofounder of Lignolix, Inc.

1. Introduction

Refined petroleum products have progressed from fuels to aromatic and olefin building blocks for the synthesis of many valuable products,[1,2] and throughout this sustained petrochemical evolution, fundamental discoveries have provided feedstocks for the large-scale production of now-ubiquitous materials such as plastics, rubbers, commodity chemicals, pharmaceutical precursors, and solvents.[2,3] These innovations have enabled significant advances in nearly every aspect of society and have supplied inexpensive bulk materials to support considerable quality-of-life improvements. Although major benefits of the petrochemical industry include economies of scale and low material costs, numerous factors may eventually necessitate a decreased reliance on virgin petroleum resources.

First, there are several environmental effects associated with petroleum processing. Aside from the greenhouse gas impacts of petroleum burned for energy,[4,5] the utilization of certain drilling and fracturing techniques can lead to increased hazards.[6,7] The extraction, refinement, and transportation of harvested petroleum also generate significant waste and volatile organic compounds, which can impact human health.[8] Materials produced from petroleum-based sources are linked to an increase in ecological pollution, as a large portion of commodity polymers are non-degradable and remain in the environment for extended periods of time.[2,9] Of the estimated 6.3 billion tons of plastic waste manufactured through 2015, nearly 80% remains in landfills or the environment, as these polymers often are cost-prohibitive to recycle or reprocess.[2,9] Second, the non-renewable nature of petrochemicals coupled with the continued demand for oil-derived products implies that petrochemical alternatives will be necessary. For example,

British Petroleum estimates that accessible worldwide reserves contain roughly 50 years of petroleum at current production levels.[10] Third, geopolitical considerations suggest a move away from petroleum reliance may be prudent. With approximately 70% of natural oil reserves located in the 13 countries affiliated with the International Organization of Petroleum Exporting Countries, the effect of geopolitical events on oil price volatility emphasizes the appeal of petroleum independence.[10–12] Overall, the petrochemical revolution has provided the raw materials necessary for societal development throughout the 1900s and early 2000s; yet, given the environmental and socioeconomic factors related to petroleum refinement and the accumulation of non-degradable and non-reprocessable waste materials derived from petrochemicals, biomass alternatives are attractive and potentially renewable targets that can be pursued.

Plant biomass is a renewable resource that constitutes ~80% of the 550 billion tons of carbon available.[13] As a major component of plant matter, lignocellulosic biomass (LCB) is the most abundant raw material on the planet, generated at over 170 billion metric tons per year as of 2010.[14,15] In the United States alone, ~1 billion tons per year of dry biomass is available, which highlights its enormous potential as a petroleum alternative.[16] This fact has not been lost on government agencies. For example, the U.S. Energy Security and Independence act of 2007 called for the annual production of nearly 80 billion L of second-generation biofuels by 2022, which implies roughly 62 million tons of lignin byproduct.[17] Despite significant efforts in the processing, chemical modification, and use of LCB as fuel alternatives, cellulosic ethanol production targets have consistently fallen short of the goals outlined in 2007.[18] This shortfall provides an opportunity in which the increased value of lignin byproducts could further promote economic competitiveness of biofuels from LCB.

Although polymers derived from renewable plant matter often are considered inherently ‘green’, it is crucial to recognize that bio-based chemicals do not intrinsically impart reduced environmental impact. For example, biopolymers have been demonstrated to better adhere to ‘green design’ principles in comparison to petroleum counterparts; yet these bio-derived macromolecules rank below several common petrochemical plastics (*e.g.*, polyolefins) in environmental impacts upon consideration of a full life-cycle analysis.[19] Despite these findings, lignin-based compounds are an excellent candidate to offer greenhouse gas mitigation in comparison to many petroleum-based chemicals.[20] Future collaboration between industry, academia, and policy regulators to assess optimal processing and manufacturing routes of lignin-based polymers could realize the potential of lignin in this regard.[20,21] Thus, the development of lignin-based macromolecules is of substantial interest, and extensive effort has been focused on the synthesis of these bio-based materials.

In this review, we highlight current research trends in the generation of bio-based materials from lignin biomass. Although several reviews have focused on lignin processing,[22] lignin deconstruction or depolymerization,[23,24] and polymerization of lignin-derivable compounds,[25] here we present a view of the translation of bulk lignin and lignin-derivable molecules into valuable polymeric systems. A survey of lignocellulose processing and lignin deconstruction is introduced, followed by a discussion of strategies for the chemical grafting of bulk lignin and the polymerization of compounds potentially obtained from lignin. These methods are categorized by polymer class, polymerization technique, and network type. Lastly, challenges and future opportunities in lignin valorization are described from technical and economic standpoints.

2. LCB

2.1 LCB structure

Lignocellulose is a complex network of carbohydrates and aromatics polymers that acts as the main support system in plants.[14,15] Structurally, LCB is comprised of three major building blocks: cellulose, hemicellulose, and lignin.[14] The exact composition of these components varies on the basis of plant species. Cellulose and hemicellulose comprise 20–30% and 40–50% by weight of LCB, respectively, with lignin as the primary remainder.[14]

Mainly used in the paper and textile industries, cellulose is a highly crystalline, fibrillar, glucose carbohydrate that provides structural reinforcement.[26] Hemicellulose also is a carbohydrate-based polymer, yet it contributes minimal physical support because of its amorphous nature.[27] Rather, hemicellulose primarily acts as a physical barrier to prevent the enzymatic degradation of cellulose.[27] Outside of their major applications in paper and textile trades, cellulose and hemicellulose have found high-volume uses as raw materials for biofuel production.[28]

Alternatively, lignin is an aromatic heteropolymer that fills the extracellular network and crosslinks cellulose.[29–31] Lignin accounts for 20–30% of dry plant matter, which makes it the most abundant aromatic polymer on the planet.[29–31] Unlike the carbohydrate-based polymers, lignin is hydrophobic yet plays a crucial role in the ability of plants to transport water.[32] It is a three-dimensional heteropolymer comprised of monolignol linkages and is primarily formed by the oxidative coupling (*in vivo*) of *p*-coumaryl alcohol, coniferyl alcohol, and sinapyl alcohol *via* a variety of carbon–carbon (*e.g.*, β-5, 5–5) and carbon–oxygen linkages (*e.g.*, β-O-4, 5-O-4).[29,33] This enzymatic coupling results in three common structural units: *p*-hydroxyphenyl (H), guaiacyl (G), and syringyl (S).[34,35]

2.2 Processing of LCB

Most LCB applications target polysaccharide content, and thus, require the isolation or enrichment of cellulose. For example, lignin impedes the enzymatic degradation of cellulose in biorefining.[17] In the paper industry, large amounts of lignin in the product detracts from the final mechanical properties, for which the highly crystalline cellulose component is vital.[36] Hence, significant effort is invested in the separation of the various LCB components prior to use, as lignin aromatic content can lead to material discoloration, odor, and property degradation.[36]

Yet, this separation of LCB into its constituent polymers is a challenge because of the chemical and thermal stability of the LCB constituents. Several pulping routes have been developed to remove lignin and hemicellulose, such as the sulfite,[37] Kraft,[38,39] soda,[40,41] thermomechanical,[42,43] and organosolv processes.[44,45] These methods largely aim to breakdown and separate LCB with the downstream regeneration or recovery of cellulose. The sulfite[37] and Kraft[38,39] approaches rely on metal sulfites and Na_2S to break lignin–cellulose bonds, respectively. Sulfite pulping results in lignosulfonate, whereas the Kraft process yields 'black liquor', from which highly sulfonated Kraft lignin is a byproduct.[38,39] Soda pulping makes use of caustic solutions of NaOH to degrade lignin–cellulose bonds.[40,41] Thermochemical pulping involves steaming and mechanical grinding of LCB under elevated temperatures, which yields a complex mixture of products.[42,43] Organosolv lignin is prepared by the solubilization of LCB components in organic/aqueous mixtures at high temperatures and benefits from milder process conditions and lower waste accumulation.[44–49] Aside from the above methods, ionic liquid pre-treatment has emerged as a newer approach for the separation of cellulose from biomass, although many ionic liquids are not considered 'green'.[46–49] Altogether, cellulose extraction is a difficult yet necessary step in the utilization of LCB; furthermore, the nature of the processing technique has a distinct impact on the obtained lignin fraction and must be considered in the potential valorization of lignin.

Residual lignin often is considered as a waste product of pulping;[50,51] of the 50–70 million tons per year of lignin waste generated globally, only ~2–5% is used, largely as composite additives, adhesives, and concrete fillers.[14,31,52–55] Thus, the development of value-added materials from lignin waste streams has tremendous economic and environmental potential, especially with the demand for biofuels expected to increase five-fold by 2030.[56] Given that low costs are a major benefit of petroleum derivatives, valorization of LCB material, particularly the lignin content of biomass, is an attractive route towards more cost-competitive and bio-based product portfolios. However, a substantial roadblock in the use of LCB waste for

higher-value applications is the chemical and structural recalcitrance of lignin, which limits processibility and chemical reactivity.

2.3 Lignin deconstruction

The deconstruction of lignin is one route to aromatic building blocks for the synthesis of new polymers. Lignin can be classified as either native (raw) or technical lignin.[57,58] Native lignin describes the unperturbed LCB state.[57,58] Technical lignin, despite being heterogeneous, more recalcitrant, and highly disperse in comparison to its native counterpart, is significant in the valorization of biomass as it is the result of LCB processing.[57,58] Although macromolecular lignin has been modified by direct chemical transformations, a key concept in the use of lignin is deconstruction to its small-molecule (*e.g.*, monomeric) or oligomeric constituents. The resultant products contain several functional handles such as alkenes, aldehydes, and phenolic residues that provide sites for chemical modifications to impart polymerizability.[59]

Deconstruction of lignin can be categorized as thermochemical/pyrolytic, catalytic, or biological.[24] Thermochemical degradation methods typically use elevated temperatures that produce complex product mixtures.[60] Catalytic deconstruction (or sometimes depolymerization) can employ organic solvents in conjunction with acids, bases, metals, or ionic liquids.[14] The metal-catalyzed deconstruction of lignin have received particular focus in recent years as catalyst developments have afforded lower energy input requirements, greater product selectivity, and deconstruction efficiency.[33] Biological routes impart enzymatic degradation to break down lignin chains.[33] Several recent reviews and articles have covered the topics of lignin deconstruction.[14,16,24,33,60]

Generally, lignin deconstruction results in three major aromatic motifs: G, S, and H.[61] The exact degradation composition can vary on the basis of plant source and deconstruction method. Lignins from softwood species (*e.g.*, cedar, pine) are dominated by G residues that contain a single *o*-phenol methoxy substituent.[14] Conversely, hardwood lignins (*e.g.*, oak, beech) contain higher S content with 2,6-dimethoxy substitutions.[14] Herbaceous lignins (*e.g.*, ferns, grasses) are comprised of various degrees of S, G, and H units.[62]Fig. 1 includes an overview of lignin formation, processing and blending routes and, deconstruction products, along with a scheme for the preparation of monomers from lignin.

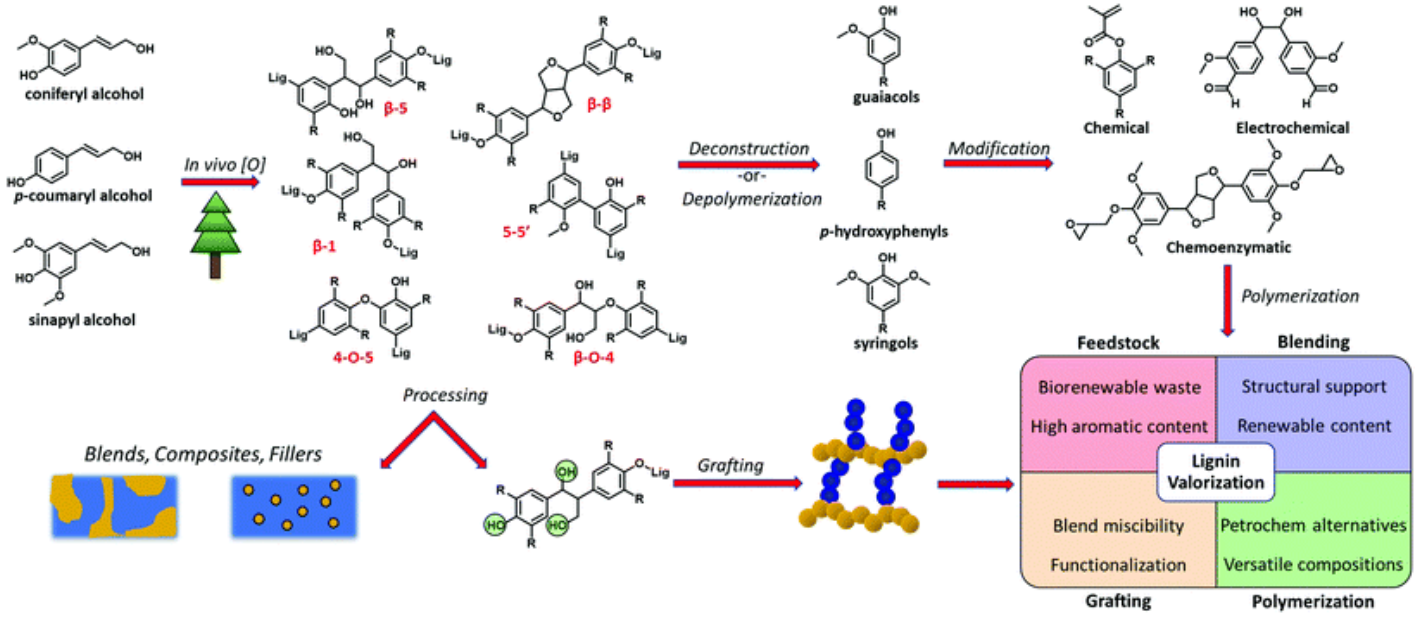

Fig. 1 From plants to polymers: an overview of the formation, processing, grafting, and deconstruction/depolymerization of bulk lignin, along with synthetic transformations to prepare monomers from deconstructed lignin.

The method of lignin deconstruction has a substantial impact on the resultant mixture. Added complications in the lignin deconstruction landscape arise from the biomass source and processing history, which introduce further variability into the deconstructed products. Thus, small molecules (*i.e.*, dimers) that contain bonds analogous to those found in bulk lignin often are used for deconstruction investigations. The application of these lignin model compounds in place of true biomass-derived aromatics avoids challenging purification steps, and the mechanisms of lignin deconstruction on certain bond moieties (*e.g.*, β-O-4, β-5) can be investigated.[51] Yet, it should be noted that the molecule choice is crucial in the study of these model systems, particularly in the examination of the effect of deconstruction conditions on specific lignin bonds.[51] Furthermore, the complex product mixtures obtained by deconstruction of real lignin can lead to difficult purifications. Thus, analogous LCB mixtures and actual lignin-derived products should be used, when possible, in the study of comprehensive strategies for lignin deconstruction and valorization.

3. Technical lignin blends and composites

3.1 Processing of lignin-polymer blends and composites

Lignin has been utilized primarily as a low-cost material in polymer composites and blends.[63] As with many characteristics of LCB, the thermal properties of lignin are strongly dependent on the source material

and treatment conditions. As such, the utilization of lignin-polymer blends requires detailed knowledge of the history of the input feedstock.[64] The glass transition temperatures (T_gs) of softwood lignins (T_g = 130–160 °C) generally are higher than those of their hardwood counterparts (T_g = 100–130 °C),[64] with this difference attributed to the higher G content in softwoods that leads to more accessible intermolecular hydrogen bond sites.[64] At temperatures below the T_g (T ~ 90–150 °C), lignin behaves as a thermoplastic material, whereas at elevated temperatures (T > 200 °C), significant degradation and/or crosslinking arise that can result in a thermoset network.[48,65] Thus, ~170 °C is often considered the optimal processing temperature to maximize material flow without degradation.[66,67] However, the substantial phenolic content on lignin results in a highly hydrogen-bonded network that is immiscible with many polymers, particularly with hydrophobic macromolecules such as polyolefins.[22,68] Of the polymers that demonstrate fair compatibility with lignin (*e.g.*, poly(hydroxybutyrate) (PHB),[69] poly(ethylene glycol) (PEG),[70–72] poly(vinyl pyrrolidone)[73,74]), phenolic hydrogen-bond disruption has been determined as the dominant factor in miscibility, with π–π and dipole–dipole interactions postulated as minor contributors.[72]

Given the narrow thermal processing window and incompatibility of lignin with a broad range of macromolecular materials, the preparation of homogeneous blends of lignin with other polymers is a challenge.[75] Several strategies have been employed to overcome miscibility issues, including chemical modification, addition of compatibilizers, and alternative processing methods. These concepts have been translated to lignin blends in electrospinning,[76] biomedical devices,[77,78] and 3D-printed composites,[79,80] in which lignin acts as an antioxidant, reinforcer, or binder.

3.2 Chemical modifications and stabilizers

One common method to improve lignin miscibility with poly(lactic acid) (PLA) is to modify the phenolic content. Labidi and coworkers investigated the impact of lignin acetylation on the extrusion of lignin/PLA blends.[81] As a result of disrupted hydrogen bonds in lignin, modified lignins had lower T_gs and improved compatibility in PLA blends.[81] Furthermore, the addition of acetylated lignin reduced hydrolysis of the PLA component.[81] In a related approach, Dong and coworkers employed a Mannich reaction to prepare lignin-melamine as a toughener in lignin/PLA/PEG blends.[82] The introduction of melamine units reduced lignin hydroxyl content and decreased particle sizes in the blends (Fig. 2A and B), which resulted in increased toughness and strain at break (ε_{break}) *versus* blends comprised of unmodified lignin (Fig. 2C and D).[82] Notably, the inclusion of lignin-melamine in the composites eliminated the brittle failure behavior found in

neat PLA.[82] Despite reduced Young's modulus (E_o) values in the lignin–PLA blends, the incorporation of modified lignin afforded similar ultimate tensile strength (UTS) values with enhanced ductility and impact strengths.[81,82]

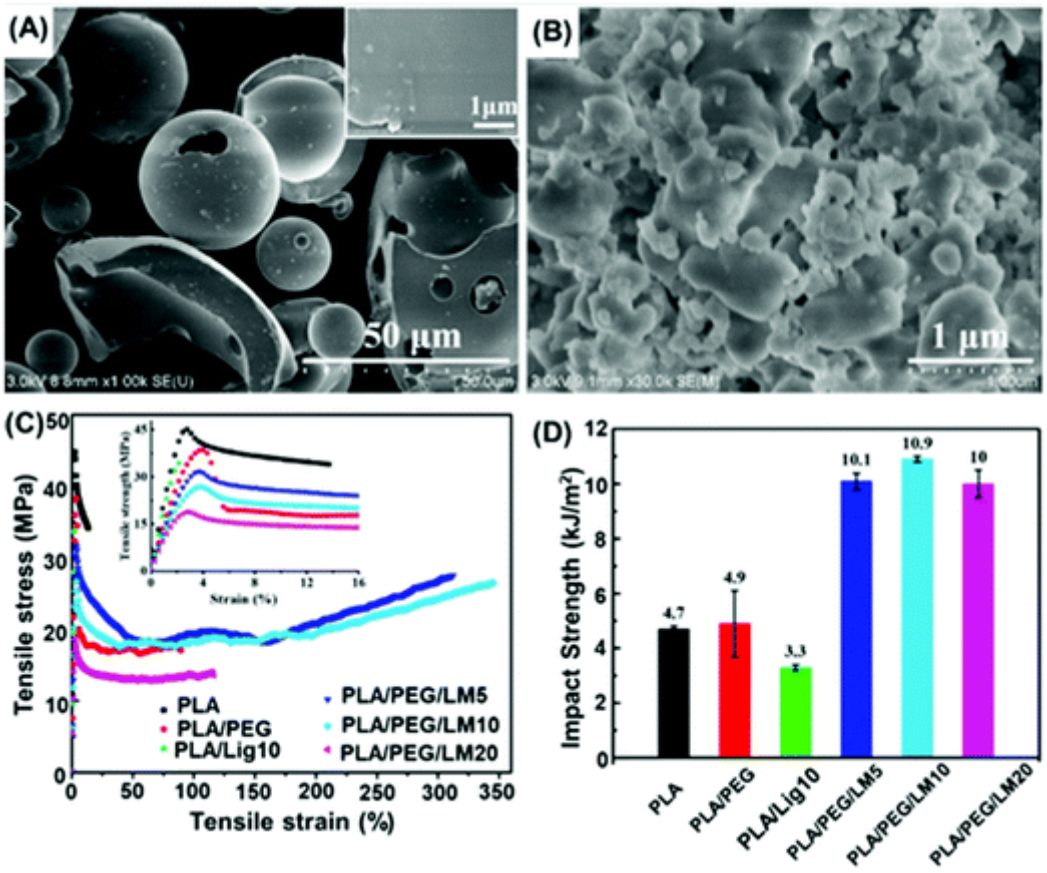

Fig. 2 Scanning electron microscopy images of (A) lignin and (B) lignin–melamine. (C) Tensile stress–strain curves and (D) notched impact strength of PLA, PLA/PEG, PLA/Lig10, and PLA/PEG/lignin–melamine at various wt% loadings. LM*x* represents *x* wt% loading of lignin or lignin–melamine. Adapted from ref. 82 with permission from Elsevier, copyright 2020.

Even though the aforementioned chemical modifications have improved blend miscibility, the processes typically require additional investments in the form of solvents, reagents, and energy inputs.[83,84] Thus, it would be advantageous to simplify the chemical transformations of lignin. Solvent-free, ball-mill transesterification was implemented as a green chemistry route to produce oleated organosolv lignin with improved miscibility in PLA/lignin blends.[83] Particle sizes of the oleated organosolv lignin (1.5–2.2 μm) were significantly smaller than those of the unmodified counterparts (14.4 μm), which facilitated improved dispersion in PLA.[83] Moreover, composites with oleated lignin had T_gs and tensile properties nearer to those of neat PLA than did samples with unmodified lignin.[83] Although the

mechanical performance of these lignin/PLA blends was similar to those of neat PLA, this solventless process afforded melt extrudability at increased lignin loadings, and it offers a strategy to increase the renewable fraction in other lignin-polymer blends.[83]

The chemical modification of lignin also has been extended to improve miscibility with other synthetic polyesters. For example, methylated lignin has been proposed as a low-cost filler for coextrusion with poly(butylene adipate-*co*-terephthalate) (PBAT).[68] Modified blends had improved tensile properties (E_o = 13.7–19.5 MPa) *versus* blends with unmodified lignin (E_o = 12.8–14.4 MPa), yet lower than that of pure PBAT (E_o = 23.7 MPa).[68] To further improve the miscibility of the system, 3 wt% PBAT grafted with maleic anhydride was added as a stabilizer, which led to more homogenous integration that provided a modulus (E_o = 18.6 MPa) closer to that of pure PBAT.[68] Despite the lowered E_o and ε_{break} values of the composite *versus* that of neat PBAT, lignin–PBAT films retained ample mechanical response for use in packaging applications, and a financial comparison indicated that the low cost of lignin afforded a 36% price reduction.[68]

Aside from its application as a low-cost filler, lignin also has been identified as a potential target to reduce the non-renewable fraction in several petrochemical-derived polymers.[85] For example, lignin has been melt-mixed with polypropylene (PP),[67,86,87] polyethylene (PE),[88] polystyrene,[89] and poly(ethylene terephthalate).[89] Blend compatibilization typically is achieved through lignin modification or the addition of a stabilizer, commonly PE or PP grafted with maleic anhydride.[67,86–88] PEG end-functionalized with aromatic acids and alkyl groups also has been an effective reactive compatibilizer in lignin-PP blends.[90] Incorporation of the compatibilizer at 2 wt% increased the impact strength, bending strength, and E_o by ~60%, ~40%, and ~20%, respectively, in comparison to blends without a compatibilizer.[90] In a similar strategy, Rodrigue and coworkers reported the modification of commercial poly(styrene-*b*-(ethylene-*co*-butylene)-*b*-styrene) for use as an unreactive compatibilizer to enhance the mechanical properties of Kraft lignin-PE blends.[91] Addition of the aminated copolymer at low loadings (2.5–5.0 wt%) led to increased compatibilization of lignin with high-density PE, and the E_o and UTS values of the composite approached or exceeded those of bulk PE (E_o ~ 350 MPa, UTS ~ 22 MPa) at up to 40 wt% lignin loading.[91] Again, this example demonstrates the possibility of enhanced performance with a simultaneous increase in the fraction of renewable and inexpensive filler content.

Although the chemical modification of lignin and the incorporation of stabilizers hold promise in the promotion of interfacial adhesion in lignin-polyolefin blends, melt blending often is insufficient for effective filler dispersion, resulting in poor stress transfer in the composite material.[84] In contrast to melt

blending, solid-state shear pulverization generates high shear and compressive forces well below the polymer T_g and/or melting temperature (T_m).[92] These mechanical forces cause particulate fracture, lead to chain scission events, and produce polymer radicals to form covalent linkages between otherwise immiscible polymers. This pulverization process has proven beneficial in the preparation of lignocellulose nanofiber-PP,[93] cellulose-PP/PE,[94] and starch-PE blends.[95,96] As one salient example, Torkelson and coworkers employed solid-state shear pulverization to generate Kraft lignin/PP and Kraft lignin/low-density PE blends.[84] The composites exhibited increased E_o and hardness values with yield strengths (σ's) that resembled those of native PE (σ = 10.0 MPa) and PP (σ = 32.0 MPa) for all formulations tested (5–30 wt% lignin);[84] however, a decrease in the ε_{break} was noted for both PP and PE composites with 20–30 wt% lignin content.[84] Nonetheless, this work highlights the vital impact of processing technique in the fabrication of lignin–polyolefin blends.[84]

In general, tradeoffs arise in lignin blends between performance, cost, and renewable fraction. The immiscibility of lignin with many polymers, especially those that are hydrophobic, leads to inadequate dispersion and often detracts from one or more mechanical properties. However, subsequent increases in other performance traits (*i.e.*, lower E_o with enhanced ductility in PLA) can prove advantageous. Although often inefficient in lignin-polymer systems, melt blending has benefitted from chemical modifications of lignin and the addition of stabilizers to enable the incorporation of relatively high lignin fractions. Alternative processing techniques, particularly solid-state shear pulverization, also have provided more homogeneous mixtures and enhanced mechanical performance, but are best at lower lignin fractions (*i.e.*, below ~30 wt%). Overall, investigation into lignin-polymer blends has demonstrated good progress, yet future work could better leverage the combination of synthetic modifications, stabilizer additives, and alternative processing strategies.

3.3 Applications of lignin-polymer blends

Aside from applications as filler materials, lignin has been used in oxidation-resistant blends,[97] biomedical devices,[98] electrospun fibers,[99] and 3D-printed biocomposites.[100] Lignin phenolic groups are structurally reminiscent of common radical scavengers (*e.g.*, butylated hydroxytoluene).[101] As such, antioxidant properties have been investigated in lignin extracted with supercritical CO_2,[102] ethanol and alkaline solvents,[103] and by enzymatic degradation.[104] For example, melt-extruded PP blends with 1–10 wt% lignin had increased oxidation induction times in comparison to neat PP at 180 °C;[97] however, an inverse correlation was found between oxidation induction time and lignin number-average molecular mass (M_n),

phenolic content, and particle size.[97] In a related study, Argyropoulos and coworkers found that the oxidation induction temperatures of neat PE (206 °C) were improved with the addition of 5 wt% softwood Kraft lignin (260 °C).[105] Interestingly, fully methylated lignin had no antioxidant properties, yet imbued the specimens with an increased oxidation induction temperature over PE blends at 5 wt% lignin (216 °C), possibly as a result of lignin char formation.[105] These efforts hint at the promise of lignin but also suggest that optimization of lignin source, composition, and degradation is required to maximize antioxidant activity.

The intrinsic antioxidant ability of lignin also has proven useful in composite hydrogels for biomedical applications.[106] For instance, lignosulfonate has been incorporated in poly(vinyl alcohol)-chitosan composites as a wound dressing, and specimens with 10 wt% lignin had enhanced hydrophilicity, protein adsorption, antimicrobial behavior, and antioxidant capability *in vitro*.[98] The three-component composite hydrogel exhibited improved tensile properties (ε_{break} = 300%, UTS = 44.3 MPa) *versus* hydrogels without lignin (ε_{break} = 200%, UTS = 38.6 MPa) and alleviated the rapid fracture of PVA-chitosan samples (Fig. 3a and b). This finding was attributed to lignin deformation before strain-induced crystallization could occur in PVA domains (Fig. 3c).[98] In another example, Yang and coworkers used a Mannich reaction to impart amine functionalities on lignosulfonate to install poly(vinyl alcohol)-reactive sites.[107] Silver nanoparticles introduced into the composite hydrogel provided enhanced antibacterial activity against *E. coli* and *S. aureus* with retention of lignin antioxidant activity.[107]

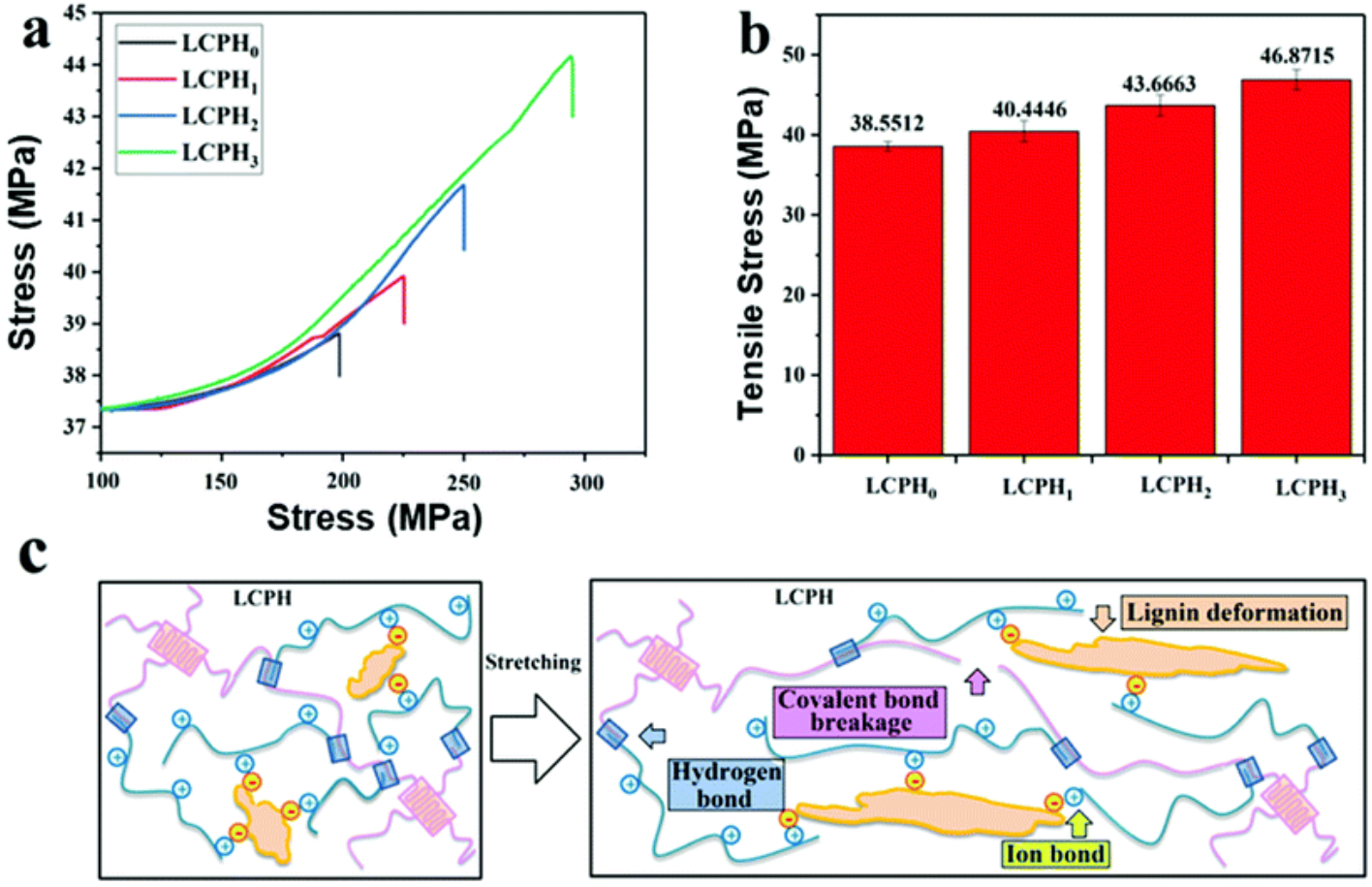

Fig. 3 (a) Compressive stress–strain curves and (b) tensile moduli of lignin-poly(vinyl alcohol)-chitosan composite hydrogels (LCPHs). (c) Proposed tensile mechanism of lignin composites demonstrating lignin deformation and structural reinforcement through hydrogen bonding. LCPH0, LCPH1, LCPH2, and LCPH3 represent composites with 0, 10, 20, and 30 wt% of lignin, respectively. Adapted from ref. 98 with permission from Elsevier, copyright 2019.

Outside of hydrogels, PEG–lignin blends have been prepared as a polymer matrix for nanocellulose composites.[108] The incorporation of 30 wt% lignin increased the shear modulus of the composite (835 kPa) *versus* that of neat PEG (442 kPa) as determined by lap-shear tests.[108] Similarly, PEG–lignin blends have been electrospun as a potential route to prepare carbonized nanofibers.[99] Although lignin contains high-carbon content beneficial for the fabrication of carbonaceous materials, lignin solutions typically lack the viscoelasticity necessary for electrospinning.[99] To overcome this hurdle, Misra and coworkers electrospun Kraft lignin complexed with different molecular weights of PEG.[99] Fibers with 5000 kDa PEG were successfully fabricated at up to 97 wt% of lignin, whereas 200 kDa PEG solutions were limited to lower lignin content (85 wt%) in the fiber production.[99] Expanding upon this work, Ko and coworkers prepared melt-spun fibers from Kraft lignin and 1000 kDa PEG.[109] Complex mechanical trends arose on the basis of

lignin type, and increased PEG content generally resulted in decreased brittleness (*i.e.*, increased ε_{break}); however, the thermal stability of the blend also was reduced.[109] Of the formulations tested, hardwood Kraft lignin:1000 kDa PEG at an 85 : 15 wt% ratio had uniform fiber diameters, stability under thermal ramping to 250 °C at 30 °C h^{-1}, and mechanical properties (E_o = 416 MPa, UTS = 1.88 MPa, ε_{break} = 10.9%) that were adequate for applications such as the fused-deposition model printing of carbon-based, nanostructured electrodes.[109] Additional investigations such as these will provide further insight into the relationship between processing conditions and blend composition with respect to fiber morphology and thermal stability.

More recently, lignin has garnered attention in protein biocomposites, which offers material fabrication from fully bioderived and possibly biodegradable materials without the need for intensive synthetic modifications or polymerizations.[100,110] For example, Kraft lignin has been used as a binder to deliver 3D-printability of fully biodegradable keratin hydrogels through 'greener' processes.[100] Lignin–keratin complexes were formed in aqueous solution and precipitated by acidification with acetic acid.[100] A 1 : 4 wt% ratio of lignin : keratin provided optimal processing conditions, as low lignin loadings maintained aqueous solubility and thermal stability during fabrication.[100]

Other plant-based proteins such as the corn biorefinery byproduct zein have been applied in 3D-print resins,[111] as bio-based thermoplastic alternatives,[112] and as a flame-resistant and insulator material.[113] However, fabrication challenges and weak mechanical strength have hindered zein's expanded application in 3D printing.[114] Bharti and coworkers demonstrated the utility of dealkaline lignin as a binding agent with zein in composite inks.[114] Granular lignin particles imparted shear-thinning behavior for enhanced printability (Fig. 4a).[114] Lignin contents up to 60 wt% reinforced the composite mechanical properties (E_o = 3.9 MPa), after which granule aggregation resulted in diminished modulus values.[114] The material inflated under vacuum at the T_g of zein (T_g = 150 °C), which also suggested the composite as a possible bio-based polystyrene foam packing alternative (Fig. 3b).[114] Furthermore, the composite was demonstrated as an insulator with thermal integrity in air up to 120 °C, which facilitated the fabrication of biodegradable circuit boards (Fig. 4c–e). Finally, the composite had considerable mass loss (80–100%) in comparison to the PLA control (25%) under microbial degradation, suggesting significant biodegradation potential.[114]

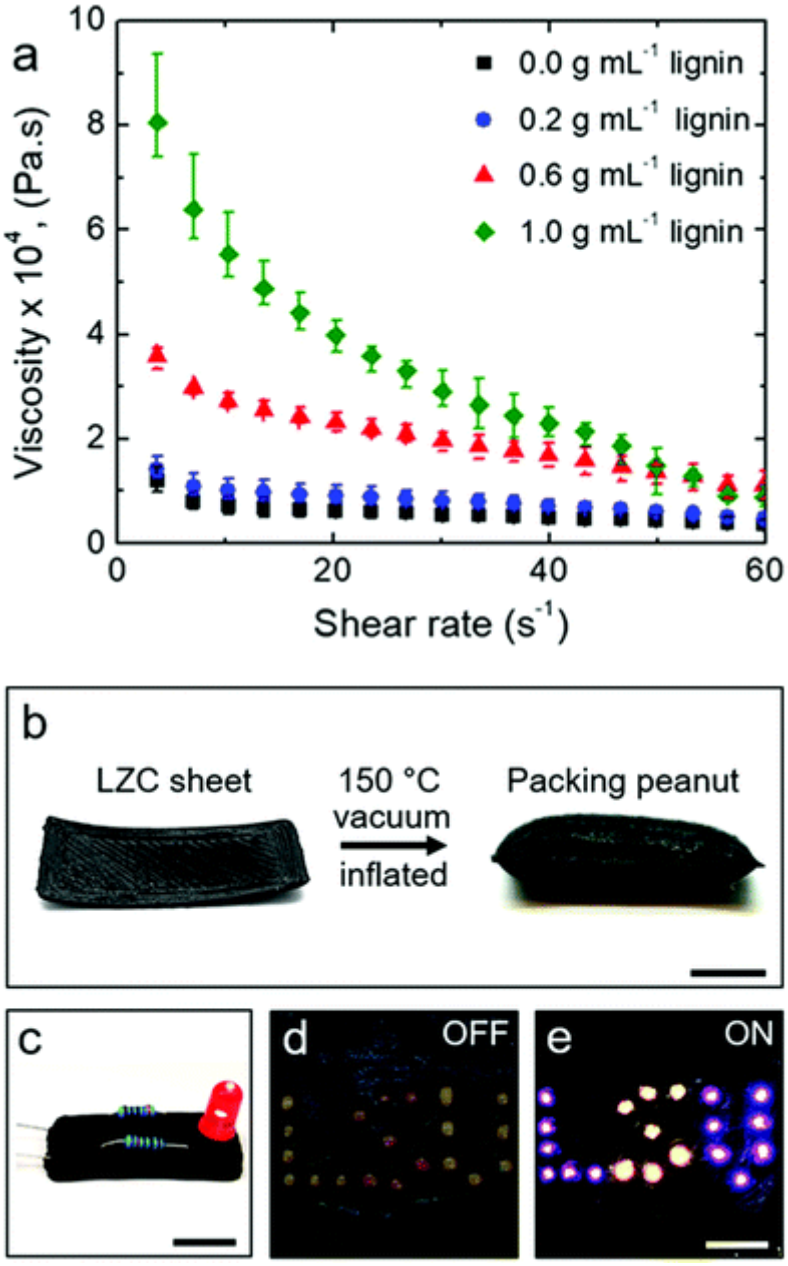

Fig. 4 (a) Complex viscosity measurements of lignin–zein composites (LZCs) as a function of lignin content. (b) Inflation of a 3D-printed LZC sheet under vacuum at the T_g of LZC. (c) LZC-embedded light-emitting diode. LZC circuit board with an external power source (d) off and (e) on. Adapted with permission from ref. 114. Copyright 2021 American Chemical Society.

Although most strategies aim for optimal blend interactions, the immiscibility in lignin-based composites can be beneficial for certain applications. As one example, biorefined softwood lignin has been incorporated as a non-reactive filler in the fused-deposition model 3D printing of PHB.[115] Blended material exhibited minimal decomposition up to 200 °C, and PHB crystallization (*ca.* 60%) was retained at all lignin loadings up to 50 wt%.[115] Moreover, composite warpage in objects printed with 50 wt% lignin

was nearly 80% lower than in pure PHB.[115] This reduced deformation was attributed to micro-voids between filler-matrix interfaces, and it underlines the potential for lignin composites in extrusion-based additive manufacturing.[115]

4. Polymer grafting and crosslinking of technical lignin

In addition to the investigation of lignin as an inexpensive and renewable blend fraction, bulk lignins have been used as macromolecular scaffolds for the synthesis of graft copolymers in reinforced nanocomposites,[116] antioxidant and ultraviolet (UV)-resistant materials,[117–119] gene therapy vehicles,[120] water purification agents,[121–123] and biomedical devices.[124,125] Polymeric branches typically are prepared *via* grafting-from, grafting-to, or grafting-through approaches.[126–128] Grafting-from involves the polymerization of monomers from initiator sites on a polymeric backbone.[126–128] Grafting-to entails the formation of covalent linkages between the pre-formed backbone and side chains, commonly *via* 'click'-type chemistry reactions.[126–129] Grafting-through utilizes tandem polymerizations such as reversible addition–fragmentation chain-transfer (RAFT) and ring-opening metathesis polymerization to synthesize and subsequently tether the macromonomers through end groups.[126–128]

The macromolecular and multifunctional nature of lignin restricts graft copolymer synthesis to grafting-from and grafting-to methods. Yet, highly branched structures can be formed through modification and/or polymerization from hydroxyl residues (grafting-from) on lignin or derivatization of these sites to produce functional handles for macromonomer attachment (grafting-to). These covalent materials can take advantage of the intrinsic properties of lignin, such as UV-resistance, antioxidant activity, and adhesive ability.[118,119] The tunability of grafts on the basis of copolymer composition, graft density, and crosslink extent enables the translation of lignin-based materials into numerous applications (*e.g.*, packaging, filtration, coatings) and is a key consideration in the preparation of high-performance materials. In this section, grafting-from and grafting-to approaches are discussed in relation to the synthesis of lignin graft copolymers and crosslinked networks.

4.1 Grafting-from

Copolymers synthesized by grafting-from generally have higher side chain densities than those from the grafting-to route.[129] Typical grafting-from strategies for bulk lignin copolymers utilize native or modified phenolic residues as initiator sites.[130] For example, the hydroxyl groups on lignin have been used in ring-opening polymerization (ROP) to prepare lignin grafted with PLA,[130–133] poly(caprolactone)

(PCL),[119,134–140] PHB,[134,141] PEG,[142] and poly(oxazolines).[143] Chemical handles also can be formed through esterification, amidation, or etherification to impart reactive groups for conventional free-radical polymerization or initiator sites for controlled-radical polymerization.[123,144]

4.1.1 ROP. The ROP of lactide from lignin has afforded lignin-*g*-PLA as tougheners[130] and UV-absorbers.[130,131] In one example, dodecylated lignin-*g*-PLA was an effective film reinforcer that provided improved mechanical properties (E_o = 2.36–3.04 GPa, UTS = 33.2–40.2 MPa, ε_{break} = 2.2–214%) *versus* neat PLA (E_o = 2.33 GPa, UTS = 28.7 MPa, ε_{break} = 5.5%).[130] In another instance, He and coworkers investigated blends of poly(L-lactic acid) (PLLA) and lignin grafted with a rubbery PCL-*co*-PLLA inner block and a PLLA or a stereocomplexing poly(D-lactic acid) (PDLA) outer block.[145] The composite materials with 5–10 wt% of grafted lignin had greater E_o, UTS, ε_{break}, and toughness values than did neat PLLA.[145] Lignin with an outer PDLA block outperformed its counterpart with an outer PLLA block as a result of complexation between PDLA and bulk PLLA.[145] Nanocomposite hydrodynamic radii (R_h) and particle sizes decreased from lignin-*g*-((PCL-*co*-PLLA)-*b*-PLLA) (R_h = 800 nm) to lignin-*g*-((PCL-*co*-PLLA)-*b*-PDLA) (R_h = 480 nm), which emphasized the effect of stereocomplexation on blend morphology as a crucial factor in the various material properties.[145]

Polyester-grafted lignins also have been explored in electrospun blends for biomedical applications. For example, lignin-*g*-PCL was synthesized by ROP of caprolactone with $Sn(Oct)_2$, and fibers were spun from a solution of PCL and the lignin copolymer.[119] The composite fibers had antioxidant behavior imparted by the lignin fraction and successfully promoted Schwann cell growth for nerve tissue engineering.[119] Lignin grafted with PCL-*co*-PLLA also has been an effective reinforcer in PCL nanofibers with improved mechanical properties (E_o = 25.9 MPa, UTS = 10.7 MPa, ε_{break} = 143%) *versus* neat PCL (E_o = 6.1 MPa, UTS = 2.9 MPa, ε_{break} = 112%).[146] The lignin-containing nanofibers were non-cytotoxic and acted as efficient scavengers of free radicals and reactive oxygen species *in vitro*, which highlights their potential to reduce oxidative stress in biomaterial applications.[133,146]

Graft architecture has been found to play a critical role in lignin–polyester composite dynamics.[134] To investigate this relationship, solutions of PHB with lignin-*g*-PHB (LPH), lignin-*g*-(PHB-*ran*-PCL) (LPHC), lignin-*g*-(PHB-*b*-PCL) (LPH + C), and lignin-*g*-(PCL-*b*-PHB) (LPC + H) were electrospun (Fig. 5A).[134] Generally, PCL domains provided interchain alignment and increased chain entanglement.[134] Furthermore, PHB segments resulted in strong interfacial interactions with the polymer matrix.[134] These individual contributions were maximized in PHB/lignin-*g*-(LPC + H) fibers, as evidenced by the improved mechanical properties of the composite (E_o = 86.1 MPa, UTS = 3.13 MPa, ε_{break} = 55%) in comparison to neat

PHB (E_o = 80.9 MPa, UTS = 1.81 MPa, ε_{break} = 15%) (Fig. 5B).[134] More specifically, the inner PCL block restricted chain mobility and improved creep resistance, and the outer PHB block provided good interfacial mixing.[134] Notably, the incorporation of lignin graft copolymers maintained cell viability and alleviated brittleness concerns of neat PHB (Fig. 5B and C).[134]

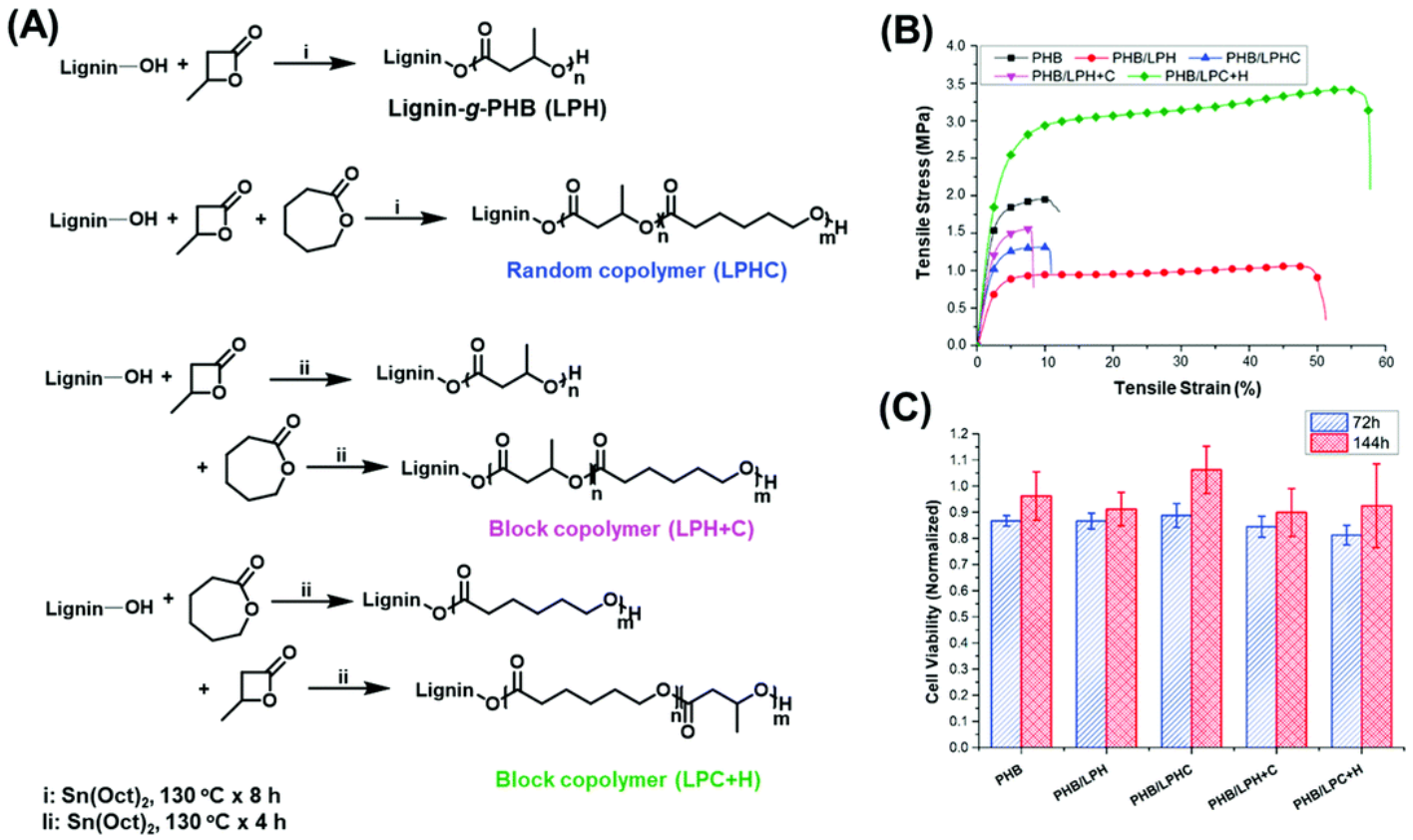

Fig. 5 (A) Synthesis of lignin-*g*-PHB (LPH), lignin-*g*-(PHB-*ran*-PCL) (LPHC), lignin-*g*-(PHB-*b*-PCL) (LPH + C), and lignin-*g*-(PCL-*b*-PHB) (LPC + H). (B) Tensile stress–strain curves of electrospun fibers of (black) PHB, (red) PHB/LPH, (blue) PHB/LPHC, (pink) PHB/LPH + C, and (green) PHB/LPC + H. (C) Cell viability of NIH/3T3 fibroblasts cultured with electrospun fibers. Adapted from ref. 134 with permission from Elsevier, copyright 2018.

ROP also has been used to graft lignin with non-polyester macromolecules.[142] As one example, poly(oxazolines) are biocompatible, peptide-like polymers that have been utilized in lignin-based hydrogels for wound dressings.[147] Mandal and coworkers prepared physically crosslinked lignin-*g*-poly(2-methyl-2-oxazoline) nanostructured gels through phenolic tosylation and subsequent cationic ROP.[143] The synthesized graft copolymers with various compositions increased in mechanical strength up to a 40

wt% lignin fraction, presumably by maximization of interpolymer hydrogen bonds between lignin and poly(2-methyloxazoline).[143] These hydrogels reduced biofilm formation, had good drug-release capability, and decreased inflammation in a rat burn model.[143] Hydrophobic lignin segments were proposed to play an essential role in the morphology and mechanical properties of the composite nanogel.

4.1.2 Radical polymerization. The development of controlled radical polymerizations such as RAFT, atom-transfer radical polymerization (ATRP), and nitroxide-mediated polymerization has enabled control over polymerization in grafting-from approaches.[148] These techniques have afforded the preparation of brush polymers with lignin as a macroinitiator.

One area of focus in lignin copolymers is the generation of bio-derivable grafts with monomers such as lauryl methacrylate and dehydroabietic ethyl methacrylate.[149,150] For example, Tang and coworkers synthesized biomass-derived lignin-soybean oil networks through RAFT polymerization of methacrylated monomers.[151] Lignin copolymers had enhanced ductility (ε_{break} = 230%) in comparison to methacrylate homopolymers (ε_{break} = 140%) and maintained thermoplastic character.[151] Moreover, epoxidation of soybean monomers with 3-chloroperoxybenzoic acid yielded an epoxy thermoset with an improved mechanical response (UTS = 17 MPa, ε_{break} = 22%) *versus* the uncured resin (UTS = 1.6 MPa, ε_{break} = 230%).[151] The ability of lignin to modulate the mechanical properties of the thermoplastic copolymer could help broaden the use of these materials in applications that require high extensibility. Additionally, thermoset network formation *via* the soybean oil fraction makes this method especially versatile to alter material characteristics in a single bio-derived system.

Bulk lignin copolymers also have been investigated as surfactants[144,152] and flocculants.[121–123] For example, RAFT polymerization of (2-methacryloyloxyethyl)trimethyl ammonium chloride (DMC) resulted in cationic flocculants with excellent removal (96.4%) of kaolin contaminants from water.[121] Xu and coworkers found lignin-*g*-PDMC to be an efficient additive in polyaluminum chloride-based flocculants.[122] Addition of the lignin copolymer improved dye removal (*ca.* 94%) in comparison to polyaluminum chloride alone (*ca.* 76–80%).[122] Furthermore, purification efficiency was retained in the presence of kaolin, which typically reduces coagulation performance.[122] The importance of inter-particle bridging on flocculation was emphasized given the increased efficacy of lignin with polymeric grafts in comparison to lignin functionalized with a single DMC monomer unit.[122] A similar strategy was used to graft *N*,*N*-dimethylaminoethyl methacrylate from lignin *via* ATRP as a switchable and CO_2-responsive emulsifier.[123] The particles successfully promoted separation of water/decane mixtures under repeated N_2/CO_2 cycles, which suggests their potential as neutral and reusable emulsifiers in pH-sensitive systems.[123] The low-

cost hydrophobic lignin fraction in these amphiphilic copolymers makes them an attractive target for large-scale applications such as wastewater treatment or oil spill remediation.

As stated previously, lignin has shown promise in biomedical applications, and lignin grafting *via* radical polymerization is another option to generate functional materials.[117,125] Loh and coworkers prepared Kraft lignin-*g*-poly(glycidyl methacrylate-*co*-(ethylene glycol)methacrylate) as a polymeric transfection alternative to poly(ethyleneimine).[120] Epoxide ring-opening by ethanolamine afforded copolymers that were effective therapeutics carriers as well as scavengers of reactive oxygen species *in vitro*.[120] Moreover, the lignin copolymers had improved cell viability *versus* poly(ethyleneimine).[120] In another example, Zhou and coworkers combined the mechanical stability and antioxidant capabilities of lignin with the bactericidal and self-healing properties of butyl-1-isopropyl-1*H*-imidazol-3-ium bromide.[117] Hydrogels fabricated by the free radical copolymerization of methacrylated-lignin, the bromide, and 2-hydroxyethylmethacrylate had a 95.6% recovery of the UTS after break ($E_{o,\ recovered}$ = 7.20 MPa), which is promising for reusable wound dressing applications.[117] From an architecture standpoint, the highly branched nature of lignin graft copolymers was beneficial in the quick gelation in hydrogel systems,[125] without a significant reduction in the self-healing capabilities of polymeric grafts.

4.1.3 Polyurethanes (PUs). PUs are a class of polymers prevalent in foams, powders, and elastomers, among other arenas.[153] PUs typically are synthesized by nucleophilic attack of polyol hydroxyls on diisocyanates (Scheme 1A). Urethane linkages can be added to lignin hydroxyls in a similar manner to prepare lignin-*g*-PU. Early work by Glasser and coworkers detailed the need for a stoichiometric excess of diisocyanates in lignin-*g*-PUs (Scheme 1B).[154] However, given the network structure of lignin, small molecule diisocyanates led to inefficient reactivity with lignin sites, which provided little remediation of the mechanical properties of bulk lignin.[154,155]

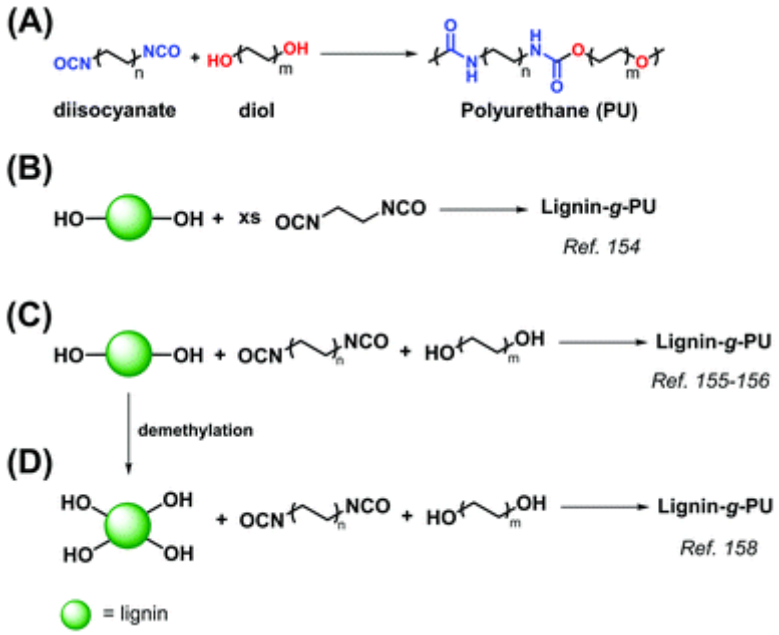

Scheme 1 (A) General reaction of a diisocyanate and a diol to form a polyurethane (PU). (B) Synthesis of lignin-*g*-PU by reaction of lignin hydroxyls and diisocyanates. Strategies to improve lignin integration in lignin-*g*-PU copolymers with a tertiary mixture of lignin/diisocyanate/diol (C) without and (D) with demethylation of the methoxy constituents.

Improved strategies in the synthesis of lignin-*g*-PU have been developed by reactions of a lignin/diisocyanate/diol tertiary mixture[155–157] (Scheme 1C) and/or by increasing the number of sites available for grafting (Scheme 1D).[155,158] For example, Washburn and coworkers demethylated lignin methoxy substituents with hexadecyltributylphosphonium bromide/HBr to provide a 28% increase in hydroxyl content for enhanced grafting efficiency.[158] A subsequent reaction of toluene diisocyanate and PEG with modified or unmodified lignin then yielded the lignin-*g*-PU.[158] The importance of adequate lignin reactivity was emphasized by the higher modulus of the demethylated lignin composite (E_o = 2.50 MPa) in comparison to that of unmodified lignin (E_o = 385 kPa) or the diisocyanate/PEG control (E_o = 230 kPa).[158]

4.2 Grafting-to

Grafting-to permits the synthesis of brush polymers with thoroughly characterized side chains prior to attachment on a macromolecular backbone. As with the grafting-from approach, this strategy has been used to incorporate co- and terpolymers onto bulk lignin.[159] One characteristic of grafting-to is the ability to generate complex and chemically variable macromonomers prior to covalent backbone attachment.[159] Although the grafting-to of lignin copolymers has received less attention than its grafting-from counterpart,

it also can afford better integration of certain polymeric classes. This strategy can be particularly advantageous in PU grafts to promote higher inter- or intra-particle crosslinking.[160] Grafting-to of lignin copolymers has been implemented in the attachment of ROP- and radical-based macromonomers, as well as in cross-linking with sulfur and thiols.

4.2.1 ROP-based macromonomers. Several approaches have been employed for the grafting-to of ROP macromonomers on lignin, such as the condensation of arylboronic acid-functionalized PCL.[161] In one example, Tang and coworkers translated a copper-free, thermally promoted azide–alkyne 'click' reaction to the synthesis of lignin grafted with PEG, PCL, and PLA as biodegradable copolymers.[159] Modulation of the T_g between −34 and 155 °C and the T_m between 38 and 55 °C was possible on the basis of polymer graft choice.[159] The use of identical 'click-to' conditions between the macromonomers highlights the versatility, experimental ease, and high-throughput potential of this route in the preparation of lignin copolymer libraries.[159]

In another grafting-to strategy, alkaline lignin recently has been implemented as a scaffold for poly(ethyleneimine)/$La(OH)_3$ in reusable nano-adsorbents to sequester phosphates.[162] A two-step synthetic procedure was performed with a Mannich reaction to graft poly(ethyleneimine) onto alkaline lignin followed by immobilization of $La(OH)_3$ under basic conditions.[162] The composite was an efficient and highly selective remover of aqueous phosphates and also retained good efficiency after three regeneration cycles (~86% of initial values).[162] Despite the fact that grafting-to of lignin with ROP macromonomers has received less attention than grafting-from, this work further explores the potential of lignin as an eco-friendly, insoluble macromolecular platform for water purification.

4.2.2 Controlled-radical polymerization-based macromonomers. Advances in controlled radical polymerization techniques have permitted the synthesis of polymers with targetable number-average degrees of polymerization (DP_ns), narrow molecular mass distributions ($Đ_m$s), and end-group fidelity useful for grafting-to incorporation.[148] For example, Liu and Chung prepared stretchable lignin-*g*-poly(5-acetylaminopentyl acrylate) nanocomposites with self-healing activity.[163] An azide-functionalized poly(acrylate), synthesized *via* RAFT polymerization, retained the end group for covalent attachment to lignin-alkyne (prepared by a Steglich esterification) through a CuBr-promoted azide–alkyne cycloaddition.[163] Copolymers with lignin loadings under 20 wt% maintained adequate flexibility to aid in hydrogen-bond-promoted self-healing.[163] Mechanical properties were strengthened with increased lignin loadings up to 20 wt% at higher graft DP_ns.[163] It was proposed that increased graft lengths resulted in a higher degree of entanglement between nanoparticles that improved mechanical stability.[163]

Furthermore, the nanocomposite had moderate self-healing 1 d after break.[163] Retention of this self-healing activity in the graft chain underlines the potential for lignin copolymers as inorganic and non-degradable filler replacements; yet, future efforts to increase the lignin fraction could prove advantageous as the synthesis of grafts generally is more costly and intensive *versus* the procurement of bulk lignin.

4.2.3 Sulfur. Commodity polymer alternatives derived from cheap, underutilized sources such as lignin and sulfur offer an attractive route to products with significant fractions of renewable content.[164] Unfortunately, bulk lignin and polymeric sulfur suffer from poor mechanical strength individually.[164] Tennyson and coworkers performed a two-step phosphorylation/allylation of alkaline lignin to impart crosslink sites for sulfur in an inverse vulcanization process (*i.e.*, sulfur as the main component).[164] Copolymers synthesized with 10–20 wt% of lignin had increased storage moduli (G' = 1.02–1.27 GPa) *versus* neat sulfur (G' = 0.37 GPa) and maintained performance after thermal reprocessing at 180 °C.[164] More recently, a radical-induced aryl halide/sulfur polymerization was implemented with the benefits of increased atom economy and process simplification.[165] Lignin chlorinated with $NaClO_3$ was crosslinked by polymeric sulfur at 230 °C to generate reprocessable materials with improved insulation in comparison to Portland Cement, which could prove beneficial in sustainable construction practices (Scheme 2).[165] Despite low lignin content in the inverse vulcanization process, these strategies offer a unique path to add value to multiple byproduct feedstocks simultaneously.

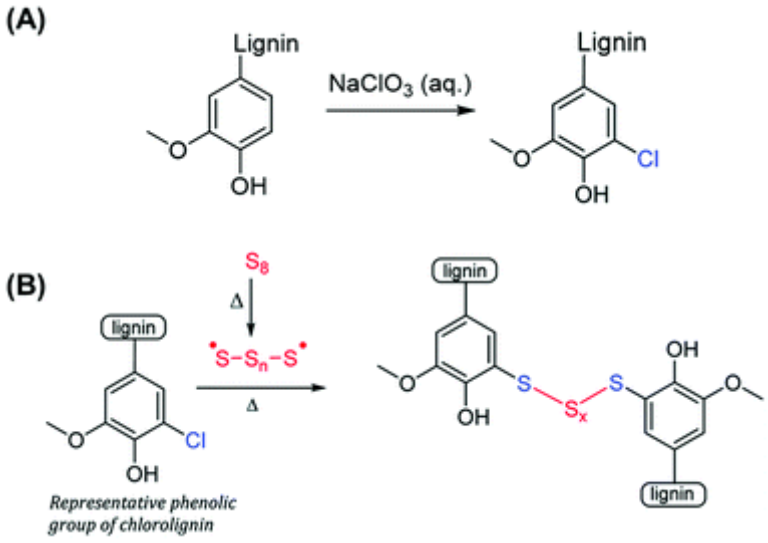

Scheme 2 (A) Preparation of chlorinated lignin using $NaClO_3$ in water. (B) Radical-induced aryl halide crosslinking of chlorinated lignin and polymeric sulfur. (B) was reproduced from ref. 165 with permission from The Royal Society of Chemistry.

Allylation of bulk lignin has further been studied to incorporate grafted crosslinks *via* thiol–ene chemistry. Lawoko and coworkers obtained fractionated Kraft lignin through extraction with ethanol and found that allylation of was efficient (>95% conversion) and highly selective for phenolic hydroxyls over aliphatic hydroxyls.[166] The T_g values of the grafted, three-arm, thiol networks (47–62 °C) largely were independent of the thiol : allyl ratios examined (0.8 : 1.0 to 1.2 : 1.0), although the broad nature of the differential scanning calorimetry (DSC) traces made precise T_g evaluation difficult.[166] This wide transition suggested a tightly formed network that resulted in a significantly higher storage modulus ($G' \sim 1$ GPa) of the thermoset *versus* typical thioether networks.[166] Additionally, the degree of crosslinker functionality (*e.g.*, 3-, 4-, 6-arm thiols) can substantially impact the thermoset morphology and thermomechanical properties of lignin-thiol networks.[167] For example, the T_g of crosslinked lignin increased from 3- (T_g = 120 °C) to 4- (T_g = 149 °C) to 6-arm thiols (T_g = 157 °C), and the G' decreased from 3- (G' = 1750 MPa) to 4- (G' = 990 MPa) to 6-arm thiols (G' = 750 MPa).[167] These moduli changes were attributed to increased looping defects and reduced stiffness in higher functionality crosslinkers.[167] Industrially relevant and scalable reactions found in these thiol–ene networks are particularly attractive as thiol crosslinkers are relatively cheap, commercially available, and can impart thermomechanical variability in a simple process.

4.2.4 PUs. Lignin-PUs synthesized *via* grafting-from typically have low integration of lignin due to low polyphenolic nucleophilicity in comparison to aliphatic polyols (*e.g.*, PEG-diol, 1,6-hexanediol).[168] One strategy to overcome this limitation is to form a lignin prepolymer with isocyanate groups (lignin-NCO) and subsequently attach polyol precursors.[169] For example, Gupta and coworkers found that soda lignin-NCO prepolymers were more amorphous than unmodified lignin, which led to better penetration and increased conversion of 400 Da PEG and methylene diphenyl diisocyanate in the lignin-*g*-PU synthesis.[168] The inclusion of lignin in the composite resulted in improved water resistance and provided densities, swelling ratios, and mechanical properties that met commercial standards for use as particleboards.[168] Eceiza and coworkers extended this strategy with southern pine Kraft lignin and isophorone diisocyanate to prepare lignin-NCO prepolymers, after which bio-based PU foams were formed by subsequent attachment of a castor oil-derived polyol (Lupranol Balance 50®, BASF).[170] Samples from lignin prepolymers had enhanced flexibility over the analogous unmodified counterparts, although their maximum energy absorption values decreased significantly.[170] The choice of unmodified or prepolymer lignin offers a balance between comfort and energy-dissipation in PU foams for personal protective equipment, and expansion of lignin-NCO prepolymer chemistries could afford high-performance materials with retention of flexibility.[170]

Oligomeric poly(butadiene) with isocyanate end groups also has been grafted on lignin to provide a rubbery block centralized between PU segments.[171] The T_g values remained constant at all wt% fractions of lignin (T_g = 150 °C), yet the moduli were 140, 15.4, and 45.1 MPa at lignin fractions of 75, 70, and 65 wt% lignin, respectively.[171] This trend was attributed to interplay between mechanical reinforcement of lignin at higher loadings (75 wt%) and increased urethane linker density at lower loadings (65 wt%), and the results emphasize the significant impact of minor variations in lignin fraction on mechanical properties.[171]

Despite progress in the grafting-to of lignin-PU copolymers,[64] the impact of diisocyanate prepolymer chemistry on lignin-PU foams largely remained unknown.[169] Biesalski and coworkers investigated the relationship of isocyanate structure and reaction efficiency of polyols and Kraft lignin functionalized with methylene, toluene, and hexamethylene diisocyanates.[169] Analysis of the cream and rise times (*i.e.*, the time when foam formation began and ended, respectively) showed faster network formation in prepolymers end-capped with isocyanates that had less steric hindrance.[169] This effect substantially impacted the macroscopic properties, as evidenced by foam collapse with the less reactive diisocyanates (*i.e.*, toluene and hexamethylene).[169] Furthermore, the compression modulus of PUs was higher with toluene diisocyanate (E_o = 1.30 MPa) in comparison to methylene diisocyanate (E_o = 0.40 MPa) and hexamethylene diisocyanate (E_o = 0.70 MPa).[169] Foam morphology and moduli differences were attributed to coagulation of unreacted lignin domains in less reactive lignin-NCO prepolymers.[169] Overall, judicious selection of diisocyanate and fabrication route can alleviate the low reactivity of lignin in PU systems.

4.2.5 Enzymatic grafting. As the *in vivo* synthesis of lignin is performed by oxidative coupling, it is feasible that the enzyme-mediated grafting of lignin copolymers could provide an environmentally friendly and highly efficient strategy without the need for direct chemical modifications of lignin. For instance, poly(acrylamide) and poly(*n*-butyl acrylate) were synthesized in ethanol/aqueous phosphate buffer with horseradish peroxidase/H_2O_2/acetylacetone as an initiator system.[172] Sequential injection of lignin generated aromatic radicals to which macromonomer grafts were coupled.[172] As another example, fully bio-based alkaline lignin-*g*-silk fibroin hydrogels have been prepared *via* laccase enzymes.[173] To fabricate the biocomposite, silk fibroin was crosslinked to lignin phenols with $(NH_4)_2S_2O_8$/$[Ru(bpy)_3]^{2+}Cl_2^{2-}$ in the presence of immobilized laccase.[173] The inherent UV-absorption properties of lignin were retained in the composite hydrogel, and the incorporation of lignin afforded a modulus (E_o = 182 kPa) nearly double that of hydrogels without lignin (E_o = 93.1 kPa).[173] Further efforts in enzymatic grafting should be explored for their one-pot potential and the capability of lignin as a reinforcer in bio-sourced protein composite hydrogels.

5. Chemical modification and polymerization of lignin-derivable monomers

The complex structure, plant source variety, deconstruction or depolymerization method, and high $Đ_m$ of biomass-derived lignin each present challenges in the use of true lignin-derived monomers. Thus, monomeric or oligomeric compounds that could potentially be obtained from lignin biomass often are employed as proxies to streamline activities associated with polymer synthesis. This commercial monomer approach represents a disconnect from actual biomass and lignin valorization efforts that is hampered by the fact that many tested monomers listed as 'lignin-derived' are of petrochemical origin and better described as potentially 'lignin-derivable'. However, it is worth noting that the 'lignin-derivable' strategy still enables the development of bulk lignin degradation and chemical valorization strategies to progress concurrently in appropriate cases.

5.1 Thermoplastic polymers from lignin-derivable compounds

A significant area of focus in the synthesis of lignin-inspired polymers is the preparation of thermoplastics with thermomechanical attributes comparable to those of commercial petrochemical-derived materials (*e.g.*, polystyrene, PMMA). This process typically proceeds by modification of phenolic residues on S, G, or H derivatives to provide polymerizable monomers.[174–176] These functionalities also allow the use of methods that would be otherwise impractical in the presence of unmodified hydroxyls (*e.g.*, radical, anionic, cationic polymerizations).[177] The library of monomers can be polymerized to probe the effect of aromatic substituents and copolymer compositions on the structure–property relationships in bio-derivable polymers,[178] especially for applications such as biomedical devices, antifouling coatings,[177] solvent-resistant films,[179] and packaging materials.[180]

5.1.1 Thermoplastics *via* chain-growth polymerization. Considerable effort has been invested in the preparation of lignin-derivable thermoplastics with thermal properties that meet or exceed those of current petrochemical options. RAFT polymerization is a common technique to synthesize these polymers in which functional handles, monomer substituent effects, and copolymer composition are significant property modifiers. As one example, Wu and coworkers polymerized syringaldehyde and vanillin with acrylate or methacrylate functionalities.[181] The T_g values ranged from 95 °C (vanillin acrylate) to 180 °C (syringyl methacrylate) with high degradation temperature (T_d) onset values (>300 °C for all polymers), which suggested the ability to tune thermal transitions on the basis of both polymerization handle and aromatic substituent.[181] These plastics had greater thermal stability *versus* other bio-based polymers (*e.g.*, PLA), and the elevated T_g of the syringyl-based polymers could be valuable in high-temperature

applications (*e.g.*, hot liquid containers). In another approach, RAFT polymerization was applied to synthesize poly(vanillin methacrylate-*b*-lauryl methacrylate) (Fig. 6A).[178] The copolymers had a low melting temperature in the lauryl methacrylate block (T_m = −33 °C) and a high T_g in the vanillin block (T_g = 120 °C), slightly above that of polystyrene (T_g = 104 °C) (Fig. 6B).[178] Small-angle X-ray scattering and transmission electron microscopy analysis indicated that the copolymer could self-assemble into classical nanostructures, such as body-centered cubic spheres (Fig. 6C).[178]

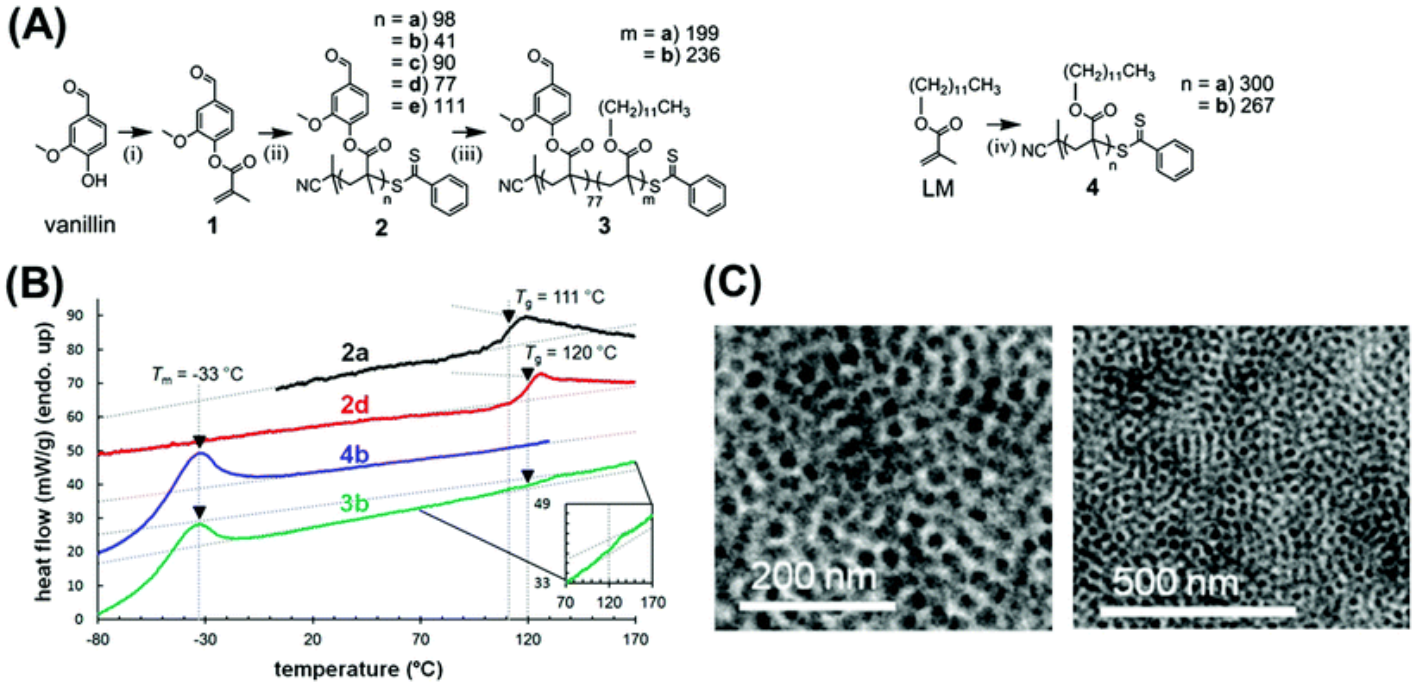

Fig. 6 (A) Synthesis of bio-based polymers from vanillin methacrylate and lauryl methacrylate (LM). Reaction conditions: (i) methacrylic anhydride, 4-dimethylaminopyridine, 55 °C. (II) chain transfer agent, 2,2′-azobisisobutyronitrile (AIBN), 1,4-dioxane for **2a–d** or anisole for **2e**, 72 °C; (iii) LM, AIBN, 1,4-dioxane for **3a** or 1 : 3 v/v 2-butanone/anisole for **3b**, 72 °C; and (iv) chain transfer agent, AIBN, 1,4-dioxane, 72 °C. (B) DSC traces of bio-based polymers on heating at 2 °C min^{-1} under N_2. (C) Transmission electron microscopy images of RuO_4-stained poly(vanillin methacrylate-*b*-lauryl methacrylate) copolymers self-assembled in a body-centered cubic morphology. Adapted with permission from ref. 178. Copyright 2014 American Chemical Society.

Lignin-inspired polymers have been synthesized by RAFT polymerization to investigate substituent effects on the viscoelastic responses and solvent-resistance properties.[180] Zero-shear viscosities in guaiacol-based polymers largely were unaffected by the alkyl substituent at the *para* position, and, in all cases, were found to be intermediate to those of polystyrene and PMMA.[180] Alternatively, the shear

modulus was substantially impacted by the alkyl group, which suggests the possibility of processability alterations without a major reduction in mechanical properties.[180] The nature of the regioisomer also has a profound impact on the properties of lignin-based polymers.[179] For example, the solvent resistance of thermoplastic films from 3,5-, 2,3-, 2,4-, and 2,6-dimethoxy phenol polymers was assessed.[179] The T_g was tunable between 82 and 203 °C on the basis of the dimethoxy isomer (2,6 > 2,4–2,3 > 3,5).[179] The higher T_g 2,6-dimethoxy polymer had enhanced solvent resistance *versus* the lower T_g 3,5-dimethoxy polymer.[179] Independent modulation of thermal transitions, viscoelastic properties, and electrophilicity in these guaiacol-based polymers on the basis of substituent and isomer exemplifies the versatility of potentially lignin-derivable monomers. For instance, isomers could prove difficult to separate in high-throughput methods (*e.g.*, distillation), and the choice of plant matter and deconstruction strategy should be considered in relation to the obtained product mixture to tailor polymer properties with minimal purification requirements.

Although most synthetic chemistry examples employ commercial monomers, recent investigations have used monomers[182] and oligomeric bio-oils[183] from deconstructed or depolymerized biomass. Acrylation of depolymerized raw poplar wood products has led to isolation of monomers such as 4-propylsyringol acrylate and 4-propylguaiacol acrylate.[182] RAFT copolymerization of these bio-sourced monomers with *n*-butyl acrylate afforded triblock copolymers with adhesive strengths (2.0–4.0 N cm^{-1}) comparable to those of commercial tapes.[182] Importantly, these values were achieved in the absence of tackifiers, which suggests that intrinsic functionalities in lignin monomers can enhance surface properties.[182]

Monomer composition can control the copolymer properties, but this approach can require multiple purifications and comonomer feeds to define the properties in the final product. Alternatively, post-polymerization modification offers the potential to create multifunctional macromolecules from a single polymeric material. For example, Maeda and coworkers translated a three-component Kabachnik–Fields reaction to vanillin and syringaldehyde polymers that allowed T_g modulation between 96 °C and 170 °C on the basis of homopolymer choice and α-amino phosphate substituent (Scheme 3).[184] The conversion of pendent aldehydes in this strategy permits late-stage property diversification in a near-quantitative and atom-economic manner, which is attractive for high-throughput screening of polymer properties and scaleup purposes (*e.g.*, continuous batch operation followed by post-polymerization derivatization).[184]

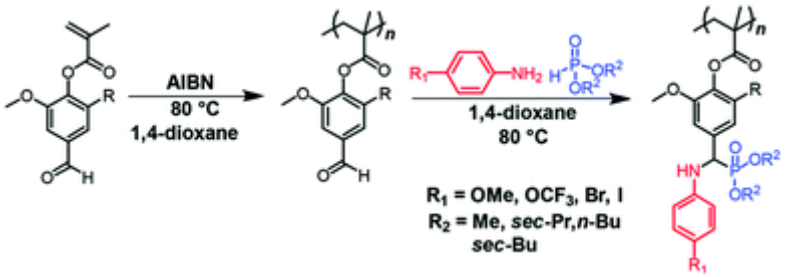

Scheme 3 Post-polymerization modification of poly(vanillin methacrylate) and poly(syringaldehyde methacrylate) *via* a three-component Kabachnik–Fields reaction. Adapted from ref. 184 with permission from The Royal Society of Chemistry.

In addition to syringyls and guaiacyls, cinnamic ester derivatives (*e.g.*, ferulic acid, caffeic acid, methyl cinnamate) have been investigated as monomers for chain-growth polymerization. The lack of emphasis on the conversion of cinnamic esters into polymeric materials partially can be attributed to the relatively low production volumes and the current utilization of these small molecules in high-value fragrances and cosmetics applications.[185,186] Although the use of cinnamic esters in personal care industries is an important application of bio-sourced aromatics, increased utilization of lignocellulose in biofuel production eventually could result in market saturation. The design of high-performance cinnamic ester-based polymers could proactively provide a direct use for excess unsaturated aromatics going forward.

One challenge is that, although these phenolic esters also benefit from unsaturated alkene substituents that permit various chemistries not easily accessible to most G and S units, cinnamic esters are not radically homopolymerizable due to steric hindrance surrounding the 1,2-disubstituted alkene.[185] Thus, they require modification or comonomers to readily generate polymers.[185] The reactivities and regioselectivities of copolymerized cinnamic ester derivatives have been explored *via* RAFT, ATRP, and nitroxide-mediated polymerization.[187] ^{1}H nuclear magnetic resonance spectroscopy of cinnamic ester products in the presence of styrenic or acrylic radicals suggested that propagation proceeded through a polystyrene-like 1,2-addition.[187] Copolymerization of *N*-isopropylacrylamide (NIPAM) and cinnamic esters provided moderate variation in the lower-critical solubility temperature range (T = 13.5–23.8 °C) that generally was increased *versus* NIPAM copolymerized with styrene.[187]

Modification of cinnamic esters also can impart homopolymerizability through both radical and ionic mechanisms (Scheme 4). Acetyl- or silyl ether-protected 4-vinylguaiacol and 4-vinylcatechol have been prepared from ferulic acid as homopolymerizable, bio-based styrenic monomers for RAFT polymerization (Scheme 4).[174] Quantitative silyl ether deprotection by HCl yielded polymers with T_gs of 110 °C for the acetylated poly(4-vinylguaiacol) and 190 °C for the poly(4-vinylcatechol).[174] A similar protecting-group

strategy was used to synthesize poly(4-vinylcatechol) by anionic polymerization with *sec*-butyl lithium as the initiator (Scheme 4).[188] Moderate tacticity control (up to rr = 79%) was achieved on the basis of solvent polarity, with syndiotactic-rich (rr = 70%) poly(4-vinylcatechol) synthesized in methylcyclohexane and isotactic-rich poly(4-vinylcatechol) produced in THF (mm = 50%).[188] This work details one of the few examples of tacticity control in the polymerization of lignin-derivable monomers to date, although the lack of crystallinity in these polymers leaves room for future advances. Overall, synthetic routes that take advantage of cinnamic ester functionalities absent in traditional petrochemical monomers have the potential to generate high-value polymers that can drive the use of these molecules outside of the cosmetic and beauty industry.

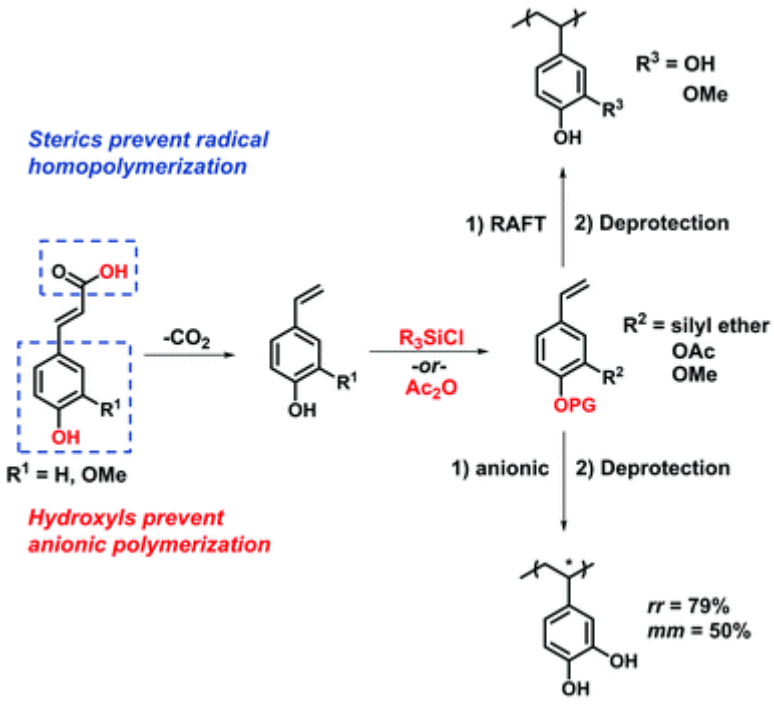

Scheme 4 Strategies to prepare homopolymerizable monomers from lignin-derivable cinnamic acids according to ref. 174 and 188.

5.1.2 Thermoplastics *via* step-growth polymerization. Step-growth polymerizations also have been examined in lignin-derivable aromatics to provide structures that more closely resemble those of petrochemical polymers such as poly(ethylene terephthalate) (*i.e.*, aromatics in the backbone).[189] These difunctional monomers typically are prepared by dimerization or condensation. This synthesis also allows for chemical variability that can afford enhanced degradation rates or additional functionality.[190]

For example, cyclic acetals have been incorporated through vanillin aldehydes to impart rigid linkers in a polymer backbone.[190] Zhang and coworkers reduced the non-renewable petrochemical fraction of poly(ethylene terephthalate)-like derivatives through the copolymerization of a vanillin spiroacetal dimer with dimethyl terephthalate and 1,6-hexanediol.[191] Although an increase in the vanillin comonomer content resulted in significantly decreased molecular masses (*e.g.*, M_n = 20, 10, and 7 kDa for 0%, 10%, and 20% vanillin), the T_g and E_o values of vanillin copolymers increased, and also, the degradability was reported to be enhanced.[191]

Aromatics such as bissyringol A (BSA), bissyringol F (BSF), bisguaiacol F (BGF), and bisguaiacol A (BGA) have been probed as low-toxicity bisphenol A (BPA) and bisphenol F (BPF) alternatives.[192–194] BSF compounds prepared by acid-catalyzed electrophilic aromatic substitution had half maximal effective concentrations 19–45× lower than BPA towards estrogen receptor α (Fig. 7A).[194] Additionally, lignin-inspired bisaromatics displayed significantly reduced estrogenic activities than those of BPA and BPF (Fig. 7B and C).[192,193] However, the T_g values of BSF polymers synthesized by step-growth condensation with terephthaloyl chloride (T_g = 157–186 °C) were considerably lower than that of the analogous BPA polymer (T_g = 226 °C).[194] Similar behavior was noted in other studies as the incorporation of methoxy substituents lowered packing efficiency, increased free volume, and reduced T_g (*e.g.*, BPA-polycarbonate (T_g = 134 °C)[195] *versus* BGA-polycarbonate (T_g = 126 °C)).[196] The nature of the bridging moiety also played a significant role on T_g. For example, the isopropylidene groups in BPA and BGA polycarbonates restricted rotational motion, and thus, materials generated from these groups had T_g values 20 °C higher than methylene-bridged analogues.[195] Although the T_g values of these syringol and guaiacol-based polymers were slightly inferior to commercial BPA and BPF benchmarks, their lower potential toxicity suggests the viability of this strategy in the future.

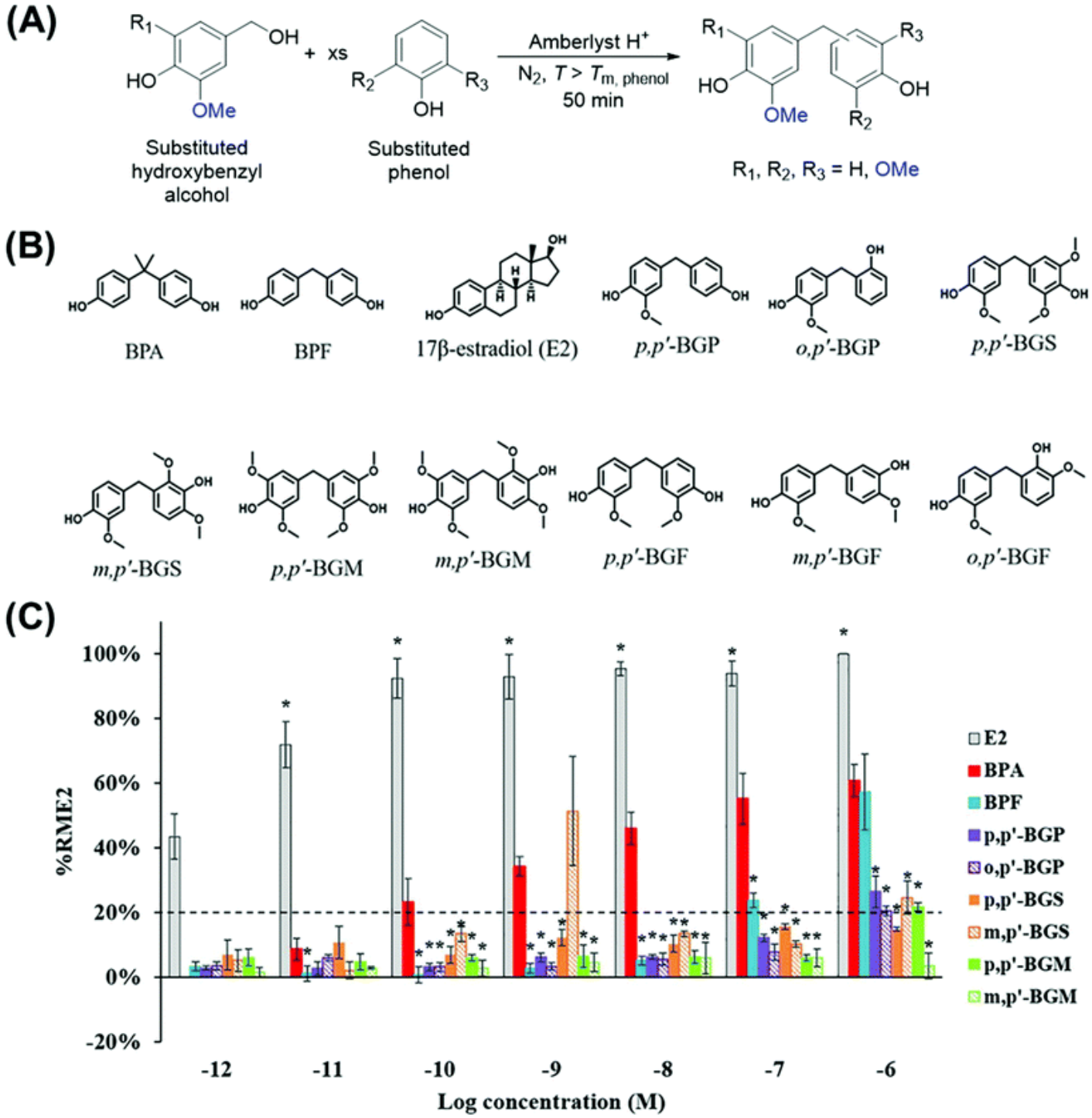

Fig. 7 (A) Electrophilic aromatic substitution of lignin-derivable bisphenols. Adapted with permission from ref. 197. Copyright 2018 American Chemical Society. (B) Structures of bisphenol A (BPA), bisphenol F (BPF), 17β-estradiol (E2), and bisphenol compounds. (C) Estrogenic activity of bisaromatics as a function of concentration. Substrates were analyzed with an MCF-7 cell proliferation assay and the percent relative maximums (%RME2) were determined with 17β-estradiol (E2) as a positive control. Figure (B) was adapted from ref. 192 with permission from Elsevier, copyright 2021. Figure (C) was reproduced from ref. 192 with permission from Elsevier, copyright 2021.

In addition to BPA alternatives, bio-inspired epoxides have been proposed as precursors for non-isocyanate PUs (NIPUs).[198–200] NIPU monomers can be prepared by dimerization, epoxidation, and subsequent formation of bis(cyclic carbonate)s (Scheme 5).[201,202] NIPU networks then can be generated *via* multifunctional amine curing (Scheme 5). This strategy avoids toxicity associated with small molecule diisocyanates and provides a 'greener' route to PU synthesis as the carbonate typically is formed using CO_2 in an atom-efficient reaction.[203,204] Thus, NIPUs have been fabricated from epoxidized soybean oil,[205] tannins,[206,207] bulk lignin,[208–210] and sunflower and castor oils[211] as isocyanate-free alternatives to PUs.

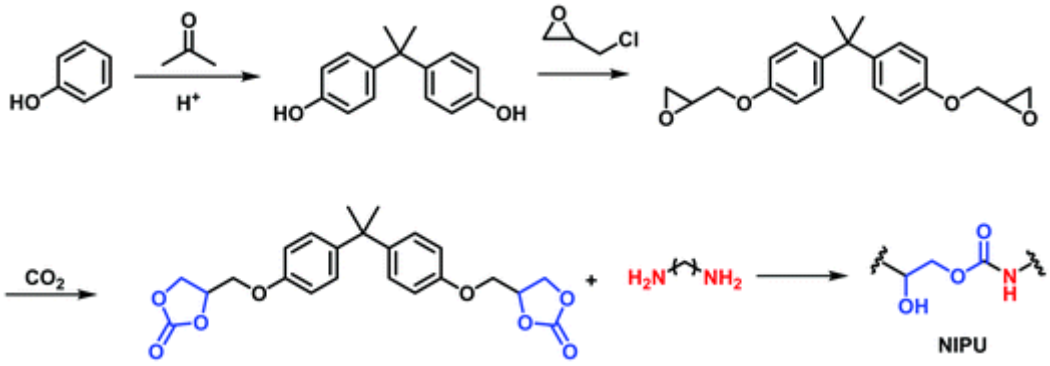

Scheme 5 Synthesis of bis(cyclic carbonates) from phenols and curing of NIPU networks with a diamine.

This synthetic approach has been extended with lignin-derivable starting materials (*e.g.*, vanillin,[212] vanillic acid,[212] ferulic acid[213]). A creosol-based bis(cyclic carbonate) recently was prepared in three steps.[214] NIPUs polymerized with 1,6-hexamethylene diamine and isophorondiamine had higher thermal transitions (T_g = 60–90 °C) than a BPA benchmark (T_g = 34 °C).[214] In another example, syringaresinol bis(cyclic carbonate)s polymerized with three different diamine hardeners had degradation characteristics ($T_{d,5\%}$ = 267–280 °C) comparable to a BPA control ($T_{d,5\%}$ = 276 °C). High char content (19–28 wt%) of the syringaresinol NIPU under N_2 *versus* a BPA NIPU (2 wt%) indicated potential application as flame-retardant materials.[199] Despite some difficulty in the synthesis of high M_n NIPUs, their production from lignin-derivable compounds offers not only a biorenewable feedstock but a 'greener' chemistry route through high conversion of CO_2 in the monomer synthesis.

5.2 Thermoset networks from lignin-derivable compounds

Thermosets form strong mechanical networks and can provide increased durability for certain applications (*e.g.*, epoxies, rubbers, photoresists, PU foams, 3D-print resins).[215] A key parameter in thermosets is the crosslink density (ν_e), which dictates structural reinforcement and impacts thermomechanical properties. As a result of their ubiquitous presence and high thermoset market share, epoxy resin alternatives constitute a significant focus for lignin-derivable compounds. The number of monomers potentially available from lignin also leaves ample room for functionalities not accessible to BPA-based epoxies. Similarly, phenol-formaldehyde thermosets are a class of high-performance aromatic networks that have applications in the construction and aerospace industries, yet given the petroleum-based nature and biological hazard of the phenol and formaldehyde monomers, both bulk lignin[65,216,217] and lignin-derivable chemicals[218] have been proposed as low-cost, sustainable, and less-toxic alternatives. In this section, recent advances are discussed with respect to lignin-inspired thermosets prepared by chain- and step-growth polymerization.

5.2.1 Thermosets *via* chain-growth polymerization. Chain-growth polymerization has been probed to generate fully bio-based lignin thermosets.[219] Liu and coworkers fabricated bio-based resins from methacrylated vanillyl alcohol (MVA) and acrylated (AESO) or methacrylated epoxidized soybean oil (MAESO) (Scheme 6).[220] Importantly, the product could be crosslinked without solvent or purification, and the use of excess methacrylic anhydride provided residual reactants in the crude mixture that could form MAESO to increase the number of available crosslink sites and improve the atom-economy (Scheme 6B).[220] Network G' and T_g values were found to increase from AESO (G' = 83 MPa, T_g = 30.1 °C) to MVA–AESO (G' = 2021 MPa, T_g = 130.8 °C) to MVA–MAESO (G' = 2110 MPa, T_g = 145.8 °C) and to MVA (G' = 2853 MPa, T_g = 180.2 °C).[220] These results were attributed to differences in ν_e as determined through dynamic mechanical analysis; ν_e was substantially lower in AESO (ν_e = 3.15 mol m^{-3}) *versus* MVA–AESO (ν_e = 7.59 mol m^{-3}) and MVA–MAESO (ν_e = 8.82 mol m^{-3}).[220] Although the full aromatic character of neat MVA had the largest G' and highest T_g, the crosslink density (ν_e = 3.34 mol m^{-3}) was near to that of AESO, likely because of imperfect network formation in these systems.[220] Nonetheless, the thermoset preparation is an attractive route as a result of (1) minimal solvent and purification requirements and (2) tunable thermomechanical properties on the basis of reactant composition in the monomer synthesis.[220]

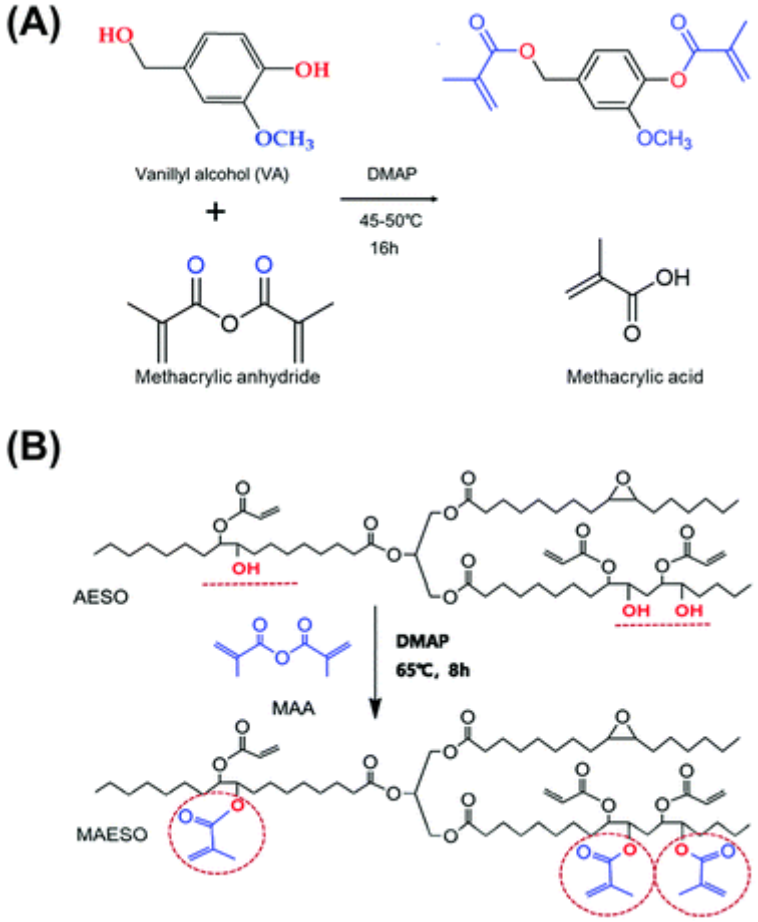

Scheme 6 Solvent-free synthesis of (A) MVA and (B) MAESO with 4-dimethylaminopyridine (DMAP) as a catalyst. Excess methacrylic anhydride (MAA) in the synthesis of MVA allowed for methacrylation of AESO to increase the number of crosslinking sites. Adapted from ref. 220. Copyright 2019 Wiley Periodicals, Inc.

Chain-growth polymerization of vanillin also has been explored for higher-value applications such as microelectronic resins with low dielectric constants (D_k).[219,221] Monomers were prepared by the reaction of triflated vanillin with bis(pinacolato)diboron, and the product was coupled to 4-bromobenzocyclobutene.[221] After alkene installation on the resultant aldehyde by reduction with CH_3PPh_3Br/*t*-BuOK, the monomer was melt polymerized through styrenic propagation and crosslinked by the strain-promoted ring-opening of the bicyclic cyclobutane (Fig. 8A).[221] The thermoset had excellent thermal resistance ($T_{d,5\%}$ = 436 °C), low moisture adsorption (0.44 wt% after 96 h in H_2O), a sufficient water contact angle (98°, Fig. 8B), and a low dielectric constant (D_k = 2.81 at 5 GHz) (Fig. 8C).[221] Despite the intensive 5-step synthesis, these thermally-polymerizable avoided the use of catalysts and additives that can negatively impact cured resin performance.[221]

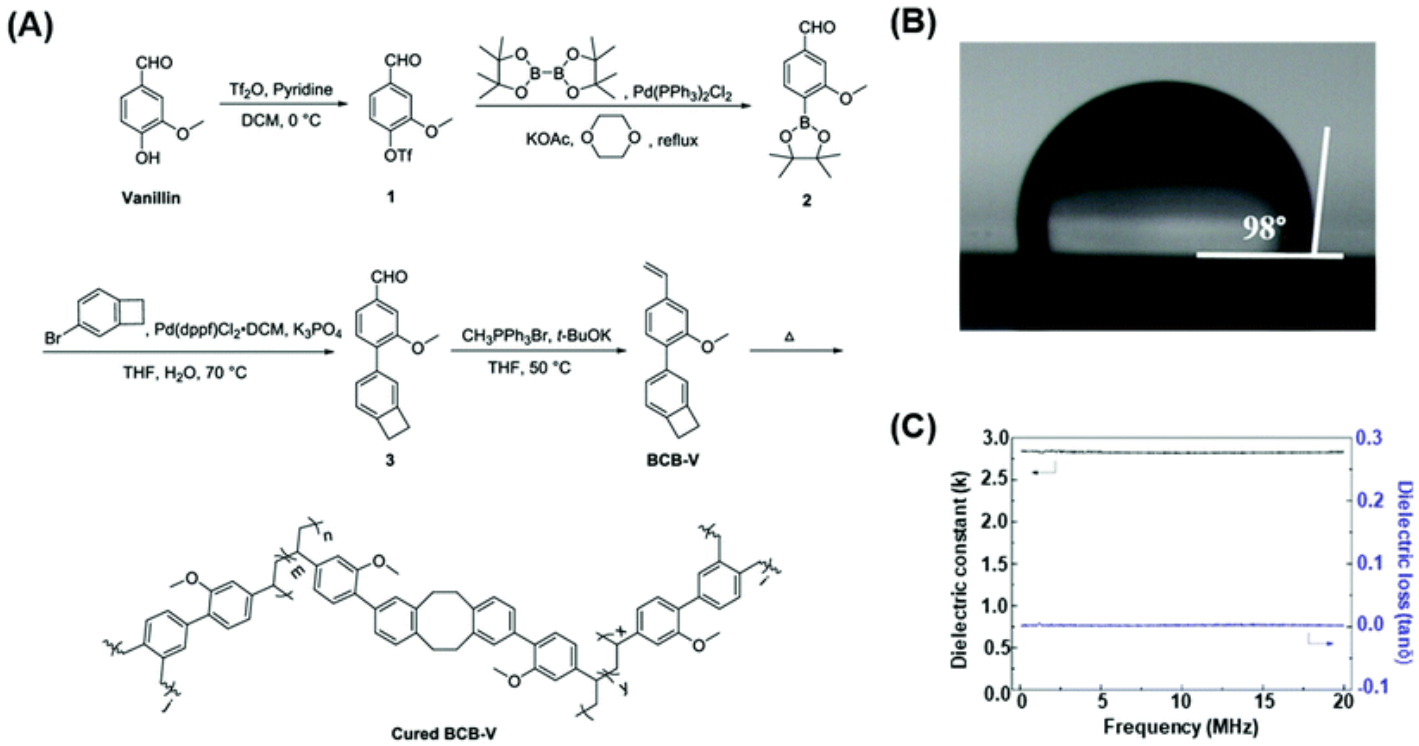

Fig. 8 (A) Synthesis, (B) contact angle, and (C) dielectric constant and loss of benzocyclobutene-vanillin (BCB-V) thermoset resins. Adapted with permission from ref. 221. Copyright 2020 American Chemical Society.

5.2.2 Thermosets *via* step-growth polymerization. Epoxies represent ~8% of the global thermosetting resin market,[215] yet 85–90% of the total epoxy share relies on BPA that carries reproductive toxicity through its estrogen-like structure.[222,223] Lignin-based thermosets provide the potential to alleviate the human and environmental health concerns, and also to impart renewability and degradability to these systems through the incorporation of labile chemistries.[224]

Functional groups found in lignin-derivable aromatics (*e.g.*, aldehydes in vanillin) bring opportunity for the attachment of degradable linkages that would be more difficult to install on BPA. 'Acid-digestible' acetal groups in glycerin-dimerized vanillin epoxides are an example of degradable linkages that can lead to the recovery of the starting materials.[225] Resins crosslinked with 4,4′-diaminodiphenylmethane had improved mechanical properties (E_o = 2.17 GPa, UTS = 105 MPa) *versus* a BPA-based analogue (E_o = 1.89 GPa, UTS = 76.4 MPa), yet retained similar thermal expansion coefficients (α_{glass} = 7.82 × 10^{-5} K^{-1} and α_{rubber} = 17.8 × 10^{-5} K^{-1} for the vanillin network; α_{glass} = 7.75 × 10^{-5} K^{-1} and α_{rubber} = 17.2 × 10^{-5} K^{-1} for the BPA network).[225] The increase in E_o and UTS were attributed to greater hydrogen-bond content in the bio-derivable system as a result of the methoxy substituent in vanillin.[225] Degradation extent also was

controllable in the vanillin networks with 0.1 M HCl in acetone : water ratios from 0 : 10 to 10 : 0, in which full degradation and no degradation were achieved, respectively.[225]

Another approach to utilize these functional groups is in resins with both epoxides and amines from lignin-derivable compounds. For example, entirely vanillin-based thermosets were prepared from vanillin epoxides and vanillin diamines.[226] Zhu and coworkers further implemented vanillin aldehydes to synthesize high-performance and intrinsically flame-resistant epoxides.[227] Condensation of a diamine and diethyl phosphate imparted thermally degradable phosphorous bonds in difunctional vanillin monomers bridged by one (EP2) or two (EP1) aromatic rings (Fig. 9A).[227] Mechanical properties of resins cured with 4,4′-diaminodiphenylmethane at 230 °C were comparable between EP1 (E_o = 2.11 GPa, UTS = 80.3 MPa, ε_{break} = 5.2%) and a BPA analogue (E_o = 1.89 GPa, UTS = 76.4 MPa, ε_{break} = 7.4%).[227] However, the EP2 network had a weaker mechanical response as the T_g (T_g = 214 °C) was nearer to the processing temperature (230 °C) in contrast to those of EP1 (T_g = 183 °C) and BPA (T_g = 166 °C) (Fig. 9B),[227] and significant internal stress in the EP2 network led to reduced mechanical performance.[227] Although the initial degradation temperatures of EP1 ($T_{d,5\%}$ = 286 °C) and EP2 ($T_{d,5\%}$ = 287 °C) networks were lower than that of the BPA benchmark ($T_{d,5\%}$ = 356 °C), the broad transitions of EP1 ($T_{d,30\%}$ = 427 °C) and EP2 ($T_{d,30\%}$ = 482 °C) were attributed to rapid degradation of labile phosphorous bonds that resulted in an insulator char layer (Fig. 9C).[227] This charring behavior could prove effective in the fabrication of flame-retardant BPA-epoxy alternatives, although the low degradation onset temperatures might limit use in high-temperature applications.[227]

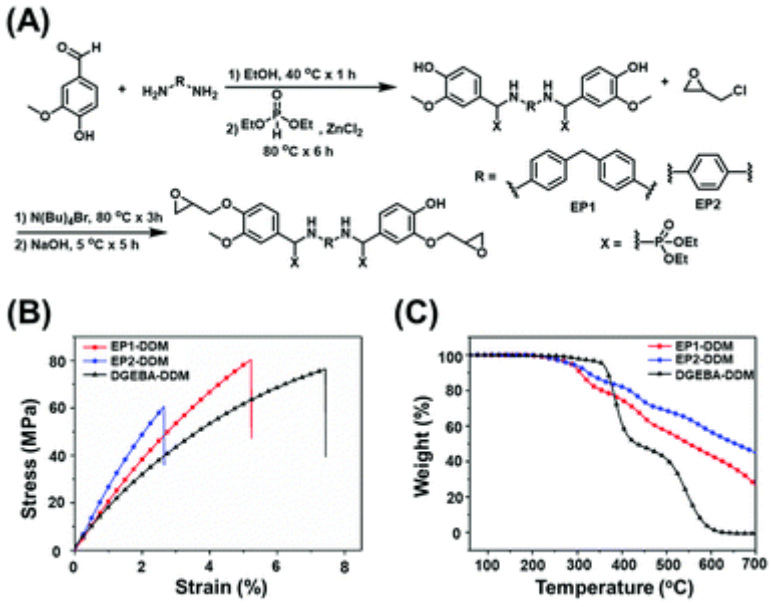

Fig. 9 (A) Synthesis of EP1 and EP2. (B) Tensile stress–strain and (C) thermogravimetric analysis (TGA) curves of (red) EP1, (blue) EP2, and (black) diglycidyl ether bisphenol A (DGEBA) cured with 4,4′-diaminodiphenylmethane (DDM). Adapted with permission from ref. 227. Copyright 2017 American Chemical Society.

Bisguaiacols also have been incorporated in thermoset networks as they offer a unique alternative to BPA epoxies in that diversity in the number and position of methoxy substituents can substantially impact network properties.[197] To probe this effect, a series of bisguaiacol epoxides with mono-, di-, tri-, and tetra-methoxy aromatic substituents were cured with 4,4′-methylenedianiline.[197] Generally, the T_g values of bisguaiacols decreased with increased methoxy content and were similar (T_g = 111–151 °C) to that of a BPF-based network (T_g = 138 °C), yet were moderately lower than that of a BPA-based specimen (T_g = 167 °C).[197] Interestingly, the regiochemistry affected the mechanical performance, as *p*,*p*′-bisguaiacols had higher *G*′ values *versus o*,*p*′- and *m*,*p*′-analogues even with the same number of methoxy substituents.[197] FT-IR spectroscopy revealed that all resins cured to similar conversions, and therefore it was proposed that the nature of the regioisomer impacted the number of network defects (*e.g.*, primary loops) during the cure process.[197]

Additional lignin-derivable bisaromatics also have been examined as BPA replacements in epoxy thermosets (*e.g.*, ferulic acid,[228–230] sinapic acid,[231] syringaresinol[232]).[21] These monomers typically show little activity towards estrogen receptor α, and thermosets derived from these compounds display thermomechanical properties similar to those of commercial BPA epoxy resins.[213,228,232] In the case of carboxylic acid-containing aromatics, curable monomers can be obtained by esterification with a diol.[228] One potential benefit of these compounds over syringol and guaiacol derivatives is the ability to modulate the polymer properties on the basis of diol linker size. For example, the glassy moduli and T_g of cured bisferulate epoxy resins were tunable across a range of alkyl spacer lengths.[228] Notably, rheological profiles of the bisferulate resins showed similar temperature dependencies to those of BPA-based analogues, which potentially suggests that these lignin-derivable aromatics could be processed in a manner similar to that of existing commercial resins.[228] Lastly, these strategies impart degradability under acidic or basic conditions, which could afford chemical recyclability not present in traditional epoxy resins.[231]

Aside from their investigation as epoxy alternatives, lignin-derivable compounds have been explored as transparent coatings. Recently, vanillin-based thermosets with fluorovinyl and poly(siloxane) linkages were

fabricated with thermally-stable crosslinks and hydrophobic *via* fluorine groups.[233] To prepare the monomer, a three-step synthesis was undertaken, with aldehyde dimerization and reduction of vanillin followed by trifluorovinyl ether installation on phenol groups.[233] Polymerization with 1,1,3,3-tetramethyl-disiloxane and a $B(C_6F_5)_3$-catalyzed Piers–Rubinsztain reaction resulted in linear chains with preservation of vinyl ethers, which subsequently could be crosslinked through a thermal [2 + 2] cycloaddition (Fig. 10A).[233] The films had high thermal transitions (T_g = 135 °C, $T_{d,5\%}$ = 385 °C) and excellent transmittance *via* UV-visible spectroscopy (Fig. 10B and C).[233] Furthermore, the storage modulus (G' = 400 MPa) of this material was significantly higher than that of crosslinked poly(dimethylsiloxane) (G' = 1–10 MPa), and the vanillin-based material prevented the acid-catalyzed degradation found in many siloxane systems.[233] Given their transparency, thermal and mechanical properties, and acid-resistance, these materials were considered as potential hydrophobic coatings.[233]

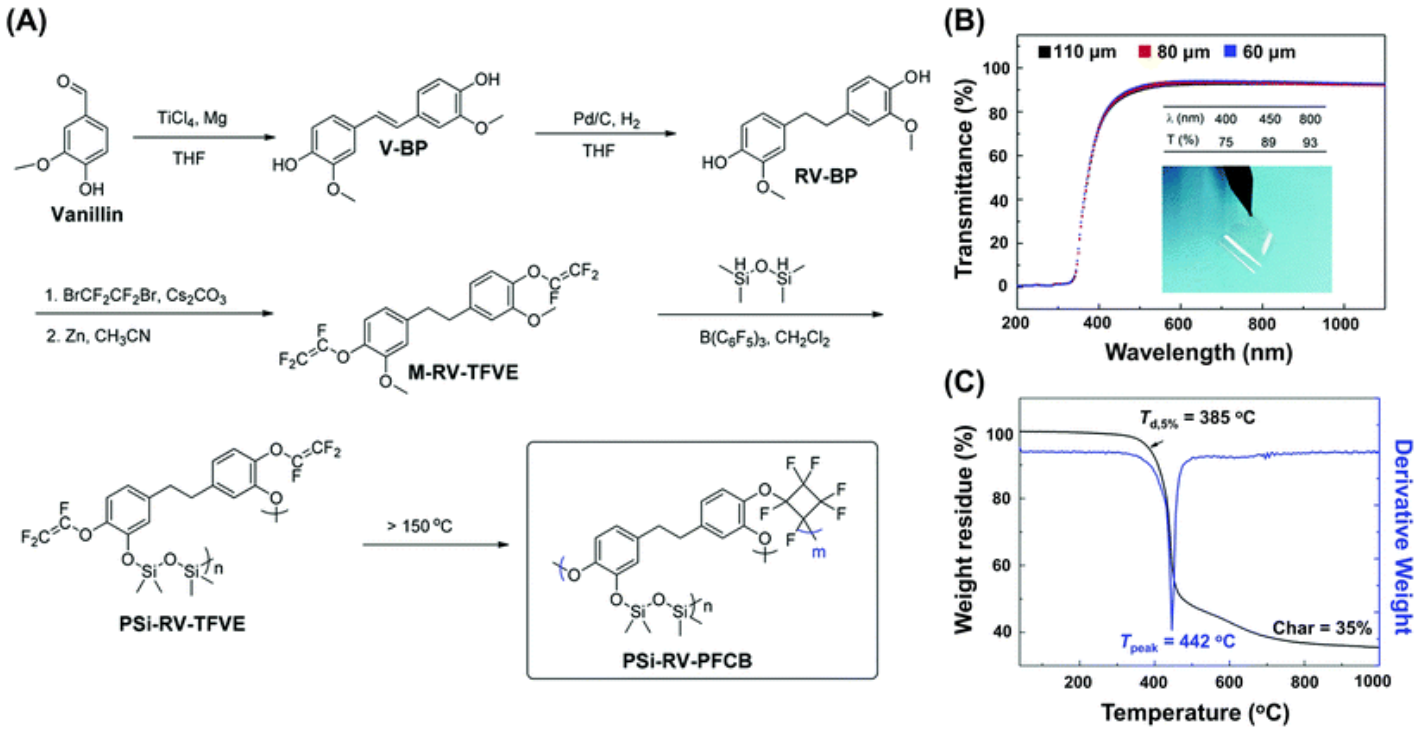

Fig. 10 (A) Synthesis, (B) TGA curve, and (C) transmittance curves of vanillin-based thermosets containing fluorovinyl ethers and poly(siloxane). Adapted with permission from ref. 233. Copyright 2019 American Chemical Society.

As previously mentioned, phenol-formaldehyde resins are another class of materials for which lignin-derivable products have been proposed as low-toxicity alternatives. For example, Caillol and coworkers

prepared phenol-formaldehyde analogues from guaiacol and terephthalaldehyde.[234] The guaiacol network was compared to commercial phenol-formaldehyde resins by dynamic mechanical analysis.[234] Although the T_g of the commercial material (T_g = 196 °C) was higher than that of the guaiacol counterpart (T_g = 164 °C), the moduli of the glassy networks (*i.e.*, $T \ll T_g$) had minimal differences (G'_{glass} = 1.6–2.8 GPa).[234] The rubbery modulus (*i.e.*, $T > T_g$) was significantly lower in the benchmark resin (G'_{rubber} = 0.04 GPa) than in the guaiacol network (G'_{rubber} = 0.61 GPa), which suggested that the latter had a higher crosslink density.[234] As a result, the tightly crosslinked guaiacol/terephthalaldehyde network was proposed as an alternative for applications such as solvent-resistant coatings; however, the lower thermal transitions need improvement to realize use in high-temperature applications.[234]

In general, these thermosets have provided thermomechanical properties suitable for alternatives to petrochemical-derived networks, particularly in epoxy resin applications. Although low yields need to be increased and/or multistep reactions often are required, these efforts highlight the potential for lignin monomers in the fabrication of renewable, less-toxic, and tunable networks in coatings, microelectronics, and intrinsically flame-resistant materials.

5.3 Vitrimers

In comparison to the mechanically robust and crosslinked structure of thermosets, melt and solvent processibility are important characteristics of thermoplastics, and tradeoffs arise between reprocessability, durability, and life cycle. Covalent adaptable networks have been developed that impart exchangeable crosslinks to address some of the limitations associated with these tradeoffs.[235] Traditional covalent adaptable network chemistries (*e.g.*, Diels–Alder) rely on dissociative exchange reactions in which bond breakage and bond formation are chemically distinct processes.[236,237] For example, bio-based furfural acetals have been incorporated into a PU copolymer that enabled dissociative acetal exchange,[238] and covalent adaptable PUs have been prepared with reversible bismaleimide Diels–Alder crosslinks in furan-PU networks.[239] In these cases, the bond breakage and bond formation are divergent steps, and thus, rate constants of the two reactions have different temperature dependencies.[236,237] Additionally, bond breakage reactions are often favored at higher temperatures, which can result in dissociative networks that suffer from losses in thermomechanical performance due to reprocessing.[236,237]

Vitrimers offer a different associative network strategy that maintains crosslink density yet can achieve thermoplastic-like flow.[240] This phenomenon occurs by stimulus-activated (*e.g.*, temperature, solvent, light) exchange reactions in which interpolymer bonds are simultaneously cleaved and reformed.[237,241–

[243] Vitrimers can make use of otherwise adverse side reactions in synthetic polymer chemistry. For example, catalyst-promoted transesterification in the synthesis of polyesters typically leads to uncontrollable M_n and broad $Đ_m$ values;[244] however, this reaction is widely employed in vitrimer chemistry as the transesterifications can retain constant crosslink densities under network rearrangement.[215] Although the field of bulk lignin vitrimers has garnered preliminary investigation,[245,246] preparation of vitrimers from lignin-derivable small molecules also has been pursued.

As one example, eugenol-epoxide dimers have been prepared through a two-step substitution/epoxidation in good overall yield (*ca.* 70%) as components in bio-based epoxy vitrimers (Scheme 7A).[247] Epoxides were cured with succinic anhydride with $Zn(acac)_2$ as a catalyst at eugenol : succinic anhydride molar ratios of 1.0 : 0.5, 1.0 : 0.75, and 1.0 : 1.0.[247] DSC results indicated that each ratio provided nearly identical T_gs (42–47 °C), whereas dynamic mechanical analysis demonstrated a decreased G' as the monomer ratios increased towards stoichiometric amounts.[247] Stress relaxations were slowest in the intermediate ratio sample, which was attributed to restricted transesterification due to the reduced availability of free eugenol epoxide hydroxyls and succinic anhydride carboxylates.[247] Only the epoxy with the highest eugenol content was amenable to physical recycling by hot pressing as a result of slow transesterification at high succinate loadings.[247] However, residual Zn^{2+} in the network allowed for chemical recycling of each network in the presence of ethanol.[247] Lastly, the epoxy networks were investigated for shape memory properties and had shape fixity and shape recovery ratios of >88% and >99%, respectively.[247]

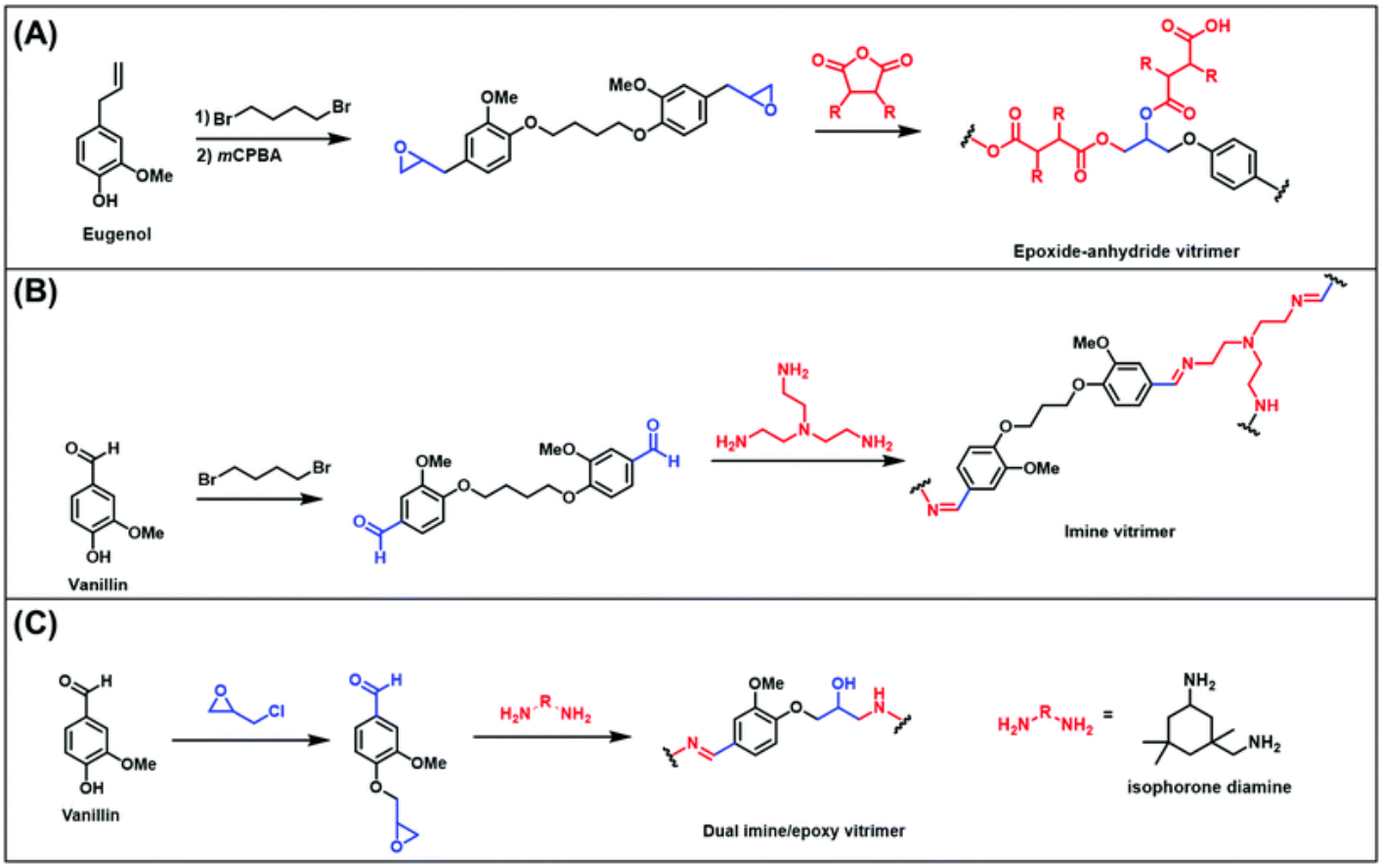

Scheme 7 Strategies to prepare vitrimers from lignin-derivable compounds with (A) epoxide-anhydride, (B) imine, and (C) dual imine/epoxy linkages.

Although the above work demonstrated the importance of monomer ratios in the preparation of recyclable lignin-based epoxy vitrimers, lower T_g values may preclude their use as potential BPA alternatives. To increase the T_g towards that of commercial epoxy systems, a triepoxy was prepared through the *p*-toluenesulfonic acid/$ZnCl_2$-catalyzed condensation of guaiacol and vanillin followed by epoxidation with epichlorohydrin.[223] Dicyclic 4-methylcyclohexane-1,2-dicarboxylic anhydride was chosen as a cure agent, and the T_gs of the resulting networks were ~180 °C.[223] These T_gs were comparable to that of a commercial BPA epoxy network (T_g = 150 °C) and also provided adequate thermal stability to prevent degradation at reprocessing temperatures ($T_{d,5\%}$ > 300 °C).[223]

Imines represent another class of vitrimer chemistry that, unlike epoxy/anhydride networks, relies on Schiff base rearrangements. Ye and coworkers prepared vitrimer films through the Schiff base polycondensation of dimerized vanillin with diethylenetriamine as a monomer and tris(2-aminoethyl)amine as a crosslinker (Scheme 7B).[248] The prepared films had high conversions with a <4 wt% soluble fraction and had similar UTS values (UTS = 47.4–57.1 MPa) and enhanced toughness (ε_{break} =

13.0–16.3%) in comparison to analogous terephthalaldehyde polyimine vitrimers (UTS = 40 MPa, ε_{break} = 5%).[248] To demonstrate network self-healing, samples were fractured and re-formed using a hot-press.[248] Despite a slight decrease in the moduli after recovery steps, the UTS and ε_{break} generally were maintained through 3 cycles.[248] The vanillin dialdehyde monomer was completely recoverable under acidic conditions (pH = 2) and successfully used in subsequent film preparation.[248] Similar Schiff base approaches in the synthesis of vanillin vitrimers with phosphorous content also have been explored as solvent-healable films,[249] bio-based flame retardants,[250] and metal adhesives.[251]

In contrast to the above strategies that utilize epoxy or imine vitrimer chemistry, a dual-functional strategy has been employed by the epoxidation of vanillin with epichlorohydrin to yield a monomer with both aldehyde and epoxide handles (Scheme 7C).[252] Although most epoxy vitrimers require additives to promote transesterification (*e.g.*, Zn^{2+}), this network was envisioned with dynamic imine linkages in addition to traditional C–N epoxy bonds from the nucleophilic ring-opening of epoxides.[252] Cured resins of the vanillin epoxide and isophorondiamine had both imine and epoxide bonds, as noted by FT-IR spectroscopy analysis.[252] DSC and TGA results indicated that the thermal properties of the network (T_g = 109 °C, $T_{d,5\%}$ = 222 °C) were near those of a commercial E51 resin (T_g = 117 °C, $T_{d,5\%}$ = 227 °C).[252] The vanillin-based resin also had mechanical responses comparable to those of the commercial resin (E_o = 2.30 GPa, UTS = 76.7 MPa) after 3 reprocessing cycles, despite some extensibility loss, virgin (ε_{break} = 4.4%) *versus* after the first recycle (ε_{break} = 3.4%).[252] Although few studies have investigated lignin-derivable vitrimers, vitrimer chemistry holds potential to extend the lifetime and reprocessibility in these bio-based systems. Future efforts could focus on the improvement of current lignin-based vitrimer chemistry or the incorporation of new adaptable network strategies to further the potential for lignin in reprocessable systems.

6. Challenges and future opportunities in lignin valorization

6.1 Challenges in lignin valorization

A typical engineering conundrum is that a project can be good, fast, or cheap; however, improvements in one area typically arise at the expense of another.[253] To provide a feasible alternative to petrochemical polymers, materials from lignocellulosic biomass must at the very least offer economic, performance, environmental, and/or throughput advantages. Although research efforts on bulk lignin and lignin-derivable compounds have produced materials with thermomechanical properties comparable to those of current plastics, a transition from the current petrochemical infrastructure requires either that (1)

regulations accelerate a shift from petroleum or (2) polymers derived from lignocellulosic biomass exhibit superior performance or longer-term (socio)economic advantages.

Lignin offers an abundant source of natural aromatics useful in synthesizing polymers with robust properties; however, several challenges exist in the valorization of lignin for commercial applications. First, processing and deconstruction of lignocellulosic biomass results in a complex combination of products that can prove difficult to separate. Despite some opportunities to use product mixtures directly (*e.g.*, 3D printing of lignin bio-oils), many polymerization techniques are less chemically tolerant and require high monomer purity. Thus, the realization of cost-competitive petrochemical alternatives from biomass may require significant innovations in polymerization chemistry or separations. On the other hand, the development of approaches that leverage the unreactive components of deconstructed lignin may avoid these issues. For example, the non-phenolic content in deconstructed lignin could potentially act as the solvent in the methacrylation and 3D printing of bio-oils. Second, industrially relevant and economic routes for the functionalization of deconstructed lignins are required. Synthetic methods are needed that use affordable reagents, involve minimal solvents, enable scalable chemistries, produce high yields, and avoid intensive purifications. Although it often is thought that bio-sourced materials are inherently greener than petrochemical-based systems, the complexities associated with lignin-derivable compound modifications can result in an increased relative carbon footprint and detract from the overall goal of the renewables space.[21] Third, though substantial progress has been made in the conversion of lignin-derivable compounds towards industrial applications, the inherent disconnect between petroleum-derived surrogate monomers and genuine deconstruction products must be overcome. This divide likely is more evident in the polymer synthesis arena, as many biomass-derived chemicals/monomers are not, outside of rare cases such as vanillin, commercially available. The use of model compounds in deconstruction/depolymerization investigations does not account for issues such as catalyst fouling, low yields, solubility concerns, and impurities that may arise in authentic biomass, each of which may prove problematic in the translation of many chemical approaches to true biomass. Overall, the recent efforts described herein have demonstrated the ability to generate viable petrochemical alternatives from lignocellulosic biomass; however, alleviation of the above challenges is desirable to optimize lignin-based materials' utility at industrial scales.

From a policy standpoint, it appears that governmental agencies have recognized the potential for lignin valorization, along with the difficulty in the connection of academic research and commercial translation. For example, the U.S. Department of Energy notes that lignin is currently undervalued yet can represent up to 40% of biomass carbon.[254] To utilize this renewable resource, a primary goal has been to

increase the industrial relevance of lignin. In particular, the U.S. Department of Energy has emphasized the development of lignin deconstruction and promotion of the resulting products to higher-value applications.[255] Similarly, LignoCity is a cooperative effort between the Research Institutes of Sweden, academic groups, and small-to-medium-sized companies. With a focus to provide a testbed for biobased efforts, Lignocity offers cost minimization and collaboration in thrusts to commercialize lignin-derived products. Comparably, the Canadian government has established integrated research programs to develop lignin-based materials.[256] Overall, endeavors by entities such as LignoCity to bridge the gap between academic research and true lignin-derived products offer promise. With the advent of new lignin-first biorefineries,[257] these strategies may become increasingly important.

6.2 Opportunities in lignin chemistry

Aside from addressing the socioeconomic and translational hurdles in the valorization of lignin, there are ample opportunities to extend the chemistries available to generate new, high-performance materials. For instance, a large fraction of current thermoplastics synthesized from lignin-derivable compounds concentrates on radical polymerization. Although excellent progress has been made in thermomechanical tunability by variation in monomer substituent groups and copolymer compositions, radical-based polymerizations generally lack stereochemical control. Thus, the synthesis of lignin-derived polymers with diverse techniques such as anionic, cationic, and group-transfer polymerizations has potential to further expand the accessible library of available polymeric properties. Furthermore, the extension of lignin monomers into new chemistries unlocks additional lignin/polymer applications. For example, the use of 3D-printable lignin monomers offers a versatile class of resins, which is particularly beneficial as a lack of material diversity is considered a major limitation in stereolithographic printing.[258] In fact, many 3D printing resins rely on commercially available acrylates and methacrylates that do not have the ideal thermomechanical variation, biodegradation, or reprocessibility for some applications. 3D printing of lignin-based compounds (*e.g.*, eugenol, vanillyl alcohol[259]) has received recent attention, and the translation of adaptable chemistries into bio-based additive manufacturing can yield renewable, high-performance, and recyclable alternatives to the commonly used acrylates[259] and bisphenols.[260] The stereoelectronic diversity found in lignin monomers also could provide a range of 3D-print properties not accessible in traditional acrylate resins.

The ease of functionalization of the phenolic hydroxyls, aldehydes, and alkenes in lignin monomers opens significant opportunities to improve material response in the resultant polymers. Expansion of polymer architectures and copolymer compositions could deliver further tunability and allow the

translation of lignin into new frontiers. In particular, the continued development of adaptable network chemistries may prove vital to unlock the reprocessibility, degradability, and application of lignin-based polymers. Additionally, extension of these polymers to higher-value applications such as stimuli-responsive materials, nanocarriers, and self-assembling templates is pivotal in the valorization of lignin, although simplified synthetic routes, higher yields, and scalable strategies are necessary to capture the full utility of lignin in these areas. For example, lignin could prove an effective delivery vehicle for hydrophobic drugs or nucleic acids, particularly those that would have increased loadings through favorable π–π interactions. Lignin-based polymers also could provide an improvement over polystyrene in lithographic applications as they maintain higher thermomechanical stabilities and may be less prone to nanostructure deformation during processing at elevated temperatures. Although challenges must be overcome before lignin can be employed in more advanced applications, great potential exists for its utility as a cost-effective, abundant, and valuable material.

7. Conclusions

Efforts to translate lignin into high-value applications have resulted in substantial progress in recent years. On one front, the use of bulk lignin has resulted in composite materials that incorporate renewability, reduce costs, and increase functionality. Yet, current strategies must be expanded and improved to realize lignin-based macromolecules as viable alternatives to petrochemical polymers. The advent of new and efficient catalytic systems in the deconstruction of lignin provides a path forward in the synthesis of novel, high-performance, designer polymers from true biomass-derived feedstocks. Furthermore, the diverse chemical composition of lignin offers a wide scope of potential monomers that should be further explored. The integration and development of lignin processing, deconstruction, and synthetic polymer chemistry could prove crucial to yield commercial, biobased products such as adhesives, packaging plastics, biomedical devices, and stimuli-responsive materials. As such, the advancement of strategies that facilitate simple, economic, and scalable chemical transformations of lignin and its small-molecule deconstruction products are paramount to enable a feasible route for the growth of the lignin bioeconomy.

Abbreviations

%RME2	Percent relative maximums
AESO	Acrylated epoxidized soybean oil
AIBN	2,2′-Azobisisobutyronitrile
ATRP	Atom-transfer radical polymerization

BCB-V	Benzocyclobutene-vanillin
BGA	Bisguaiacol A
BGF	Bisguaiacol F
BPA	Bisphenol A
BPF	Bisphenol F
BSA	Bissyringol A
BSF	Bissyringol F
DDM	4,4′-Diaminodiphenylmethane
DGEBA	Diglycidyl ether bisphenol A
D_k	Dielectric constant
$Đ_m$	Molecular mass distribution
DMAP	4-Dimethylaminopyridine
DMC	(2-Methacryloyloxyethyl)trimethyl ammonium chloride
DP_n	Number-average degree of polymerization
DSC	Differential scanning calorimetry
E2	17β-Estradiol
E_o	Young's modulus
FT-IR	Fourier-transform infrared
G	Guaiacyl
G'	Storage modulus
H	*p*-Hydroxyphenyl
LM	Lauryl methacrylate
LCB	Lignocellulosic biomass
LPH	Lignin-*g*-PHB
LPHC	Lignin-*g*-(PHB-*ran*-PCL)
LPH + C	Lignin-*g*-(PHB-*b*-PCL)
LPC + H	Lignin-*g*-(PCL-*b*-PHB)
LZC	Lignin–zein composite
MAA	Methacrylic anhydride

MAESO	Methacrylated epoxidized soybean oil
M_n	Number-average molecular mass
MVA	Methacrylated vanillyl alcohol
NIPAM	*N*-Isopropylacrylamide
NIPU	Non-isocyanate polyurethane
PBAT	Poly(butylene adipate-*co*-terephthalate)
PCL	Poly(caprolactone)
PDLA	Poly(D-lactic acid)
PE	Polyethylene
PEG	Poly(ethylene glycol)
PHB	Poly(hydroxybutyrate)
PLA	Poly(lactic acid)
PLLA	Poly(L-lactic acid)
PP	Polypropylene
PU	Polyurethane
RAFT	Reversible addition–fragmentation chain-transfer
R_h	Hydrodynamic radius
ROP	Ring-opening polymerization
S	Syringyl
T_d	Degradation temperature
T_g	Glass transition temperature
TGA	Thermogravimetric analysis
T_m	Melting temperature
UTS	Ultimate tensile strength
UV	Ultraviolet
v_e	Crosslink density
α	Thermal expansion coefficient
ε_{break}	Strain at break
σ	Yield strength

Conflicts of interest

The authors declare no conflicts of interest.

Acknowledgements

The authors are grateful for financial support from the National Science Foundation Growing Convergence Research program (NSF GCR CMMI 1934887) in Materials Life-Cycle Management and the State of Delaware (RAPID project funding) during the writing of this manuscript.

Notes and references

1. R. J. Clews, in *Project Finance for the International Petroleum Industry*, ed. R. J. Clews, Academic Press, San Diego, 2016, pp. 83–99 Search PubMed.
2. R. Geyer, J. R. Jambeck and K. L. Law, *Sci. Adv.*, 2017, **3**, e1700782 CrossRef.
3. B. M. Upton and A. M. Kasko, *Chem. Rev.*, 2016, **116**, 2275–2306 CrossRef CAS.
4. M. S. Masnadi, H. M. El-Houjeiri, D. Schunack, Y. Li, S. O. Roberts, S. Przesmitzki, A. R. Brandt and M. Wang, *Nat. Energy*, 2018, **3**, 220–226 CrossRef CAS.
5. M. S. Masnadi, H. M. El-Houjeiri, D. Schunack, Y. Li, J. G. Englander, A. Badahdah, J.-C. Monfort, J. E. Anderson, T. J. Wallington, J. A. Bergerson, D. Gordon, J. Koomey, S. Przesmitzki, I. L. Azevedo, X. T. Bi, J. E. Duffy, G. A. Heath, G. A. Keoleian, C. McGlade, D. N. Meehan, S. Yeh, F. You, M. Wang and A. R. Brandt, *Science*, 2018, **361**, 851 CrossRef CAS PubMed.
6. P. Perez, G. Dalu, N. Gomez and H. Tan, *Saf. Reliab.*, 2018, **38**, 99–133 CrossRef.
7. Q. Meng, *Sci. Total Environ.*, 2017, **580**, 953–957 CrossRef CAS PubMed.
8. R. M. O'Dea, J. A. Willie and T. H. Epps III, *ACS Macro Lett.*, 2020, **9**, 476–493 CrossRef.
9. J. C. Worch and A. P. Dove, *ACS Macro Lett.*, 2020, **9**, 1494–1506 CrossRef CAS.
10. bp Statistical Review of World Energy 2020, https://www.bp.com/content/dam/bp/business-sites/en/global/corporate/pdfs/energy-economics/statistical-review/bp-stats-review-2020-full-report.pdf, (accessed March 2021).
11. R. L. Hirsch, *Science*, 1987, **235**, 1467 CrossRef CAS PubMed.
12. W. Matar, S. M. Al-Fattah, T. Atallah and A. Pierru, *OPEC Energy Rev.*, 2013, **37**, 247–269 CrossRef.
13. Y. M. Bar-On, R. Phillips and R. Milo, *Proc. Natl. Acad. Sci. U. S. A.*, 2018, **115**, 6506–6511 CrossRef CAS PubMed.

14. C. Li, X. Zhao, A. Wang, G. W. Huber and T. Zhang, *Chem. Rev.*, 2015, **115**, 11559–11624 CrossRef CAS PubMed.
15. T. E. Amidon and S. Liu, *Biotechnol. Adv.*, 2009, **27**, 542–550 CrossRef CAS PubMed.
16. J. Zakzeski, P. C. A. Bruijnincx, A. L. Jongerius and B. M. Weckhuysen, *Chem. Rev.*, 2010, **110**, 3552–3599 CrossRef CAS PubMed.
17. A. J. Ragauskas, G. T. Beckham, M. J. Biddy, R. Chandra, F. Chen, M. F. Davis, B. H. Davison, R. A. Dixon, P. Gilna, M. Keller, P. Langan, A. K. Naskar, J. N. Saddler, T. J. Tschaplinski, G. A. Tuskan and C. E. Wyman, *Science*, 2014, **344**, 1246843 CrossRef PubMed.
18. Q. Nguyen, J. Bowyer, J. Howe, S. Bratkovich, H. Groot, E. Pepke and K. Fernholz, *Global production of second generation biofuels: Trends and influences*, Dovetail Partners Inc, 2017 Search PubMed.
19. M. D. Tabone, J. J. Cregg, E. J. Beckman and A. E. Landis, *Environ. Sci. Technol.*, 2010, **44**, 8264–8269 CrossRef CAS PubMed.
20. M. Montazeri, G. G. Zaimes, V. Khanna and M. J. Eckelman, *ACS Sustainable Chem. Eng.*, 2016, **4**, 6443–6454 CrossRef CAS.
21. S. Fadlallah, P. Sinha Roy, G. Garnier, K. Saito and F. Allais, *Green Chem.*, 2021, **23**, 1495–1535 RSC.
22. M. N. Collins, M. Nechifor, F. Tanasă, M. Zănoagă, A. McLoughlin, M. A. Stróżyk, M. Culebras and C.-A. Teacă, *Int. J. Biol. Macromol.*, 2019, **131**, 828–849 CrossRef CAS PubMed.
23. L. Yang, K. Seshan and Y. Li, *Catal. Today*, 2017, **298**, 276–297 CrossRef CAS.
24. H. Wang, M. Tucker and Y. Ji, *J. Appl. Chem.*, 2013, **2013**, 838645 Search PubMed.
25. A. Llevot, E. Grau, S. Carlotti, S. Grelier and H. Cramail, *Macromol. Rapid Commun.*, 2016, **37**, 9–28 CrossRef CAS PubMed.
26. M. S. Singhvi, S. Chaudhari and D. V. Gokhale, *RSC Adv.*, 2014, **4**, 8271–8277 RSC.
27. J. Kruyeniski, P. J. T. Ferreira, M. G. V. S. Carvalho, M. E. Vallejos, F. E. Felissia and M. C. Area, *Ind. Crops Prod.*, 2019, **130**, 528–536 CrossRef CAS.
28. P. Dey, V. Rangarajan, J. Singh, J. Nayak and K. J. Dilip, *Biomass Convers. Biorefin.*, 2021 Search PubMed.
29. Y. Tobimatsu and M. Schuetz, *Curr. Opin. Biotechnol.*, 2019, **56**, 75–81 CrossRef CAS PubMed.
30. W. Boerjan, J. Ralph and M. Baucher, *Annu. Rev. Plant Biol.*, 2003, **54**, 519–546 CrossRef CAS PubMed.
31. M. Kleinert and T. Barth, *Chem. Eng. Technol.*, 2008, **31**, 736–745 CrossRef CAS.
32. C. Wang, S. S. Kelley and R. A. Venditti, *ChemSusChem*, 2016, **9**, 770–783 CrossRef CAS PubMed.

33. C. Chio, M. Sain and W. Qin, *Renewable Sustainable Energy Rev.*, 2019, **107**, 232–249 CrossRef CAS .
34. T. Wells, M. Kosa and A. J. Ragauskas, *Ultrason. Sonochem.*, 2013, **20**, 1463–1469 CrossRef CAS PubMed .
35. A. Naseem, S. Tabasum, K. M. Zia, M. Zuber, M. Ali and A. Noreen, *Int. J. Biol. Macromol.*, 2016, **93**, 296–313 CrossRef CAS PubMed .
36. I. Haq, P. Mazumder and A. S. Kalamdhad, *Bioresour. Technol.*, 2020, **312**, 123636 CrossRef CAS PubMed .
37. L. P. Christov, M. Akhtar and B. A. Prior, *Enzyme Microb. Technol.*, 1998, **23**, 70–74 CrossRef CAS .
38. F. S. Chakar and A. J. Ragauskas, *Ind. Crops Prod.*, 2004, **20**, 131–141 CrossRef CAS .
39. G. Gellerstedt, *Ind. Crops Prod.*, 2015, **77**, 845–854 CrossRef CAS .
40. G. Iglesias, M. Bao, J. Lamas and A. Vega, *Bioresour. Technol.*, 1996, **58**, 17–23 CrossRef CAS .
41. S. I. Mussatto, G. Dragone, G. J. M. Rocha and I. C. Roberto, *Carbohydr. Polym.*, 2006, **64**, 22–28 CrossRef CAS .
42. A. G. Vishtal and A. Kraslawski, *BioResources*, 2011, **6**, 3547–3568 Search PubMed .
43. F. Oveissi and P. Fatehi, *Environ. Technol.*, 2014, **35**, 2597–2603 CrossRef CAS .
44. T. N. Kleinert, *US Pat*, US3585104A, 1971 Search PubMed .
45. Z. Zhou, F. Lei, P. Li and J. Jiang, *Biotechnol. Bioeng.*, 2018, **115**, 2683–2702 CrossRef CAS PubMed .
46. Z. Usmani, M. Sharma, P. Gupta, Y. Karpichev, N. Gathergood, R. Bhat and V. K. Gupta, *Bioresour. Technol.*, 2020, **304**, 123003 CrossRef CAS .
47. N. Sun, H. Rodríguez, M. Rahman and R. D. Rogers, *ChemComm*, 2011, **47**, 1405–1421 RSC .
48. W. Li, N. Sun, B. Stoner, X. Jiang, X. Lu and R. D. Rogers, *Green Chem.*, 2011, **13**, 2038–2047 RSC .
49. J. Wang, R. Boy, N. A. Nguyen, J. K. Keum, D. A. Cullen, J. Chen, M. Soliman, K. C. Littrell, D. Harper, L. Tetard, T. G. Rials, A. K. Naskar and N. Labbé, *ACS Sustainable Chem. Eng.*, 2017, **5**, 8044–8052 CrossRef CAS .
50. N. Mahmood, Z. Yuan, J. Schmidt and C. Xu, *Renewable Sustainable Energy Rev.*, 2016, **60**, 317–329 CrossRef CAS .
51. C. W. Lahive, P. C. J. Kamer, C. S. Lancefield and P. J. Deuss, *ChemSusChem*, 2020, **13**, 4238–4265 CrossRef CAS PubMed .
52. W. O. S. Doherty, P. Mousavioun and C. M. Fellows, *Ind. Crops Prod.*, 2011, **33**, 259–276 CrossRef CAS .
53. E. Ten and W. Vermerris, *J. Appl. Polym. Sci.*, 2015, **132**, 42069 CrossRef .

54. M. Alekhina, O. Ershova, A. Ebert, S. Heikkinen and H. Sixta, *Ind. Crops Prod.*, 2015, **66**, 220–228 CrossRef CAS .
55. D. S. Bajwa, G. Pourhashem, A. H. Ullah and S. G. Bajwa, *Ind. Crops Prod.*, 2019, **139**, 111526 CrossRef CAS .
56. K. Lopez-Camas, M. Arshad and A. Ullah, in *Lignin: Biosynthesis and Transformation for Industrial Applications*, ed. S. Sharma and A. Kumar, Springer International Publishing, Cham, 2020, pp. 139–180, DOI:10.1007/978-3-030-40663-9_5 .
57. A. Duval and M. Lawoko, *React. Funct. Polym.*, 2014, **85**, 78–96 CrossRef CAS .
58. E. Feghali, K. M. Torr, D. J. van de Pas, P. Ortiz, K. Vanbroekhoven, W. Eevers and R. Vendamme, *Top. Curr. Chem.*, 2018, **376**, 32 CrossRef PubMed .
59. Z. Sun, B. Fridrich, A. de Santi, S. Elangovan and K. Barta, *Chem. Rev.*, 2018, **118**, 614–678 CrossRef CAS .
60. M. P. Pandey and C. S. Kim, *Chem. Eng. Technol.*, 2011, **34**, 29–41 CrossRef CAS .
61. F. G. Calvo-Flores and J. A. Dobado, *ChemSusChem*, 2010, **3**, 1227–1235 CrossRef CAS PubMed .
62. S. Zhou, Y. Xue, A. Sharma and X. Bai, *ACS Sustainable Chem. Eng.*, 2016, **4**, 6608–6617 CrossRef CAS .
63. M. Culebras, M. J. Sanchis, A. Beaucamp, M. Carsí, B. K. Kandola, A. R. Horrocks, G. Panzetti, C. Birkinshaw and M. N. Collins, *Green Chem.*, 2018, **20**, 4461–4472 RSC .
64. S. Sen, S. Patil and D. S. Argyropoulos, *Green Chem.*, 2015, **17**, 4862–4887 RSC .
65. A. Tejado, C. Peña, J. Labidi, J. M. Echeverria and I. Mondragon, *Bioresour. Technol.*, 2007, **98**, 1655–1663 CrossRef CAS PubMed .
66. Y. Tang, M. Jean, S. Pourebrahimi, D. Rodrigue and Z. Ye, *Can. J. Chem. Eng.*, 2020, 1–12 Search PubMed .
67. G. Toriz, F. Denes and R. A. Young, *Polym. Compos.*, 2002, **23**, 806–813 CrossRef CAS .
68. S.-J. Xiong, B. Pang, S.-J. Zhou, M.-K. Li, S. Yang, Y.-Y. Wang, Q. Shi, S.-F. Wang, T.-Q. Yuan and R.-C. Sun, *ACS Sustainable Chem. Eng.*, 2020, **8**, 5338–5346 CrossRef CAS .
69. P. Mousavioun, W. O. S. Doherty and G. George, *Ind. Crops Prod.*, 2010, **32**, 656–661 CrossRef CAS .
70. J. F. Kadla and S. Kubo, *Macromolecules*, 2003, **36**, 7803–7811 CrossRef CAS .
71. S. Kubo and J. F. Kadla, *J. Appl. Polym. Sci.*, 2005, **98**, 1437–1444 CrossRef CAS .
72. S. Kubo and J. F. Kadla, *Holzforschung*, 2006, **60**, 245–252 CAS .

73. M. F. Silva, C. A. da Silva, F. C. Fogo, E. A. G. Pineda and A. A. W. Hechenleitner, *J. Therm. Anal. Calorim.*, 2005, **79**, 367–370 CrossRef CAS.
74. Y. Teramoto, S.-H. Lee and T. Endo, *J. Appl. Polym. Sci.*, 2012, **125**, 2063–2070 CrossRef CAS.
75. S. Yang, T.-Q. Yuan, Q. Shi and R.-C. Sun, in *Green Chemistry and Chemical Engineering*, ed. B. Han and T. Wu, Springer New York, New York, NY, 2019, pp. 405–426, DOI:10.1007/978-1-4939-9060-3_1015.
76. E. Svinterikos, I. Zuburtikudis and M. Al-Marzouqi, *ACS Sustainable Chem. Eng.*, 2020, **8**, 13868–13893 CrossRef CAS.
77. R. Liang, J. Zhao, B. Li, P. Cai, X. J. Loh, C. Xu, P. Chen, D. Kai and L. Zheng, *Biomaterials*, 2020, **230**, 119601 CrossRef CAS PubMed.
78. I. Spiridon and C. E. Tanase, *Int. J. Biol. Macromol.*, 2018, **114**, 855–863 CrossRef CAS PubMed.
79. S. Zhang, M. Li, N. Hao and A. J. Ragauskas, *ACS Omega*, 2019, **4**, 20197–20204 CrossRef CAS PubMed.
80. J. Roman, W. Neri, V. Fierro, A. Celzard, A. Bentaleb, I. Ly, J. Zhong, A. Derré and P. Poulin, *Nano Today*, 2020, **33**, 100881 CrossRef CAS.
81. O. Gordobil, I. Egüés, R. Llano-Ponte and J. Labidi, *Polym. Degrad. Stab.*, 2014, **108**, 330–338 CrossRef CAS.
82. D. Wang, Y. Wang, W. Wang, T. Li, J. Jiang, B. Xia, P. Ma, M. Chen and W. Dong, *Compos. Commun.*, 2020, **22**, 100501 CrossRef.
83. X. Guo, X. Junna, M. P. Wolcott and J. Zhang, *ChemistrySelect*, 2016, **1**, 3449–3454 CrossRef CAS.
84. K. A. Iyer and J. M. Torkelson, *ACS Sustainable Chem. Eng.*, 2015, **3**, 959–968 CrossRef CAS.
85. C. Huang, J. He, R. Narron, Y. Wang and Q. Yong, *ACS Sustainable Chem. Eng.*, 2017, **5**, 11770–11779 CrossRef CAS.
86. C. González Sánchez and L. A. E. Alvarez, *Angew. Makromol. Chem.*, 1999, **272**, 65–70 CrossRef.
87. A. V. Maldhure, J. D. Ekhe and E. Deenadayalan, *J. Appl. Polym. Sci.*, 2012, **125**, 1701–1712 CrossRef CAS.
88. L. Hu, T. Stevanovic and D. Rodrigue, *J. Appl. Polym. Sci.*, 2015, **132**, 41484 Search PubMed.
89. H. Jeong, J. Park, S. Kim, J. Lee and J. W. Cho, *Fibers Polym.*, 2012, **13**, 1310–1318 CrossRef CAS.
90. X. Xu, Z. He, S. Lu, D. Guo and J. Yu, *Macromol. Res.*, 2014, **22**, 1084–1089 CrossRef CAS.
91. L. Hu, T. Stevanovic and D. Rodrigue, *J. Appl. Polym. Sci.*, 2014, **131**, 41040 CrossRef.
92. N. Furgiuele, A. H. Lebovitz, K. Khait and J. M. Torkelson, *Macromolecules*, 2000, **33**, 225–228 CrossRef CAS.

93. S. Iwamoto, S. Yamamoto, S.-H. Lee and T. Endo, *Cellulose*, 2014, **21**, 1573–1580 CrossRef CAS .
94. K. A. Iyer, G. T. Schueneman and J. M. Torkelson, *Polymer*, 2015, **56**, 464–475 CrossRef CAS .
95. A. M. Walker, Y. Tao and J. M. Torkelson, *Polymer*, 2007, **48**, 1066–1074 CrossRef CAS .
96. P. J. Brunner, J. T. Clark, J. M. Torkelson and K. Wakabayashi, *Polym. Eng. Sci.*, 2012, **52**, 1555–1564 CrossRef CAS .
97. C. Pouteau, P. Dole, B. Cathala, L. Averous and N. Boquillon, *Polym. Degrad. Stab.*, 2003, **81**, 9–18 CrossRef CAS .
98. Y. Zhang, M. Jiang, Y. Zhang, Q. Cao, X. Wang, Y. Han, G. Sun, Y. Li and J. Zhou, *Mater. Sci. Eng., C*, 2019, **104**, 110002 CrossRef CAS PubMed .
99. V. Poursorkhabi, A. K. Mohanty and M. Misra, *J. Appl. Polym. Sci.*, 2015, **132**, 41260 CrossRef .
100. W. J. Grigsby, S. M. Scott, M. I. Plowman-Holmes, P. G. Middlewood and K. Recabar, *Acta Biomater.*, 2020, **104**, 95–103 CrossRef CAS PubMed .
101. E. T. Denisov and I. V. Khudyakov, *Chem. Rev.*, 1987, **87**, 1313–1357 CrossRef CAS .
102. Q. Lu, M. Zhu, Y. Zu, W. Liu, L. Yang, Y. Zhang, X. Zhao, X. Zhang, X. Zhang and W. Li, *Food Chem.*, 2012, **135**, 63–67 CrossRef CAS .
103. Z. Li and Y. Ge, *Int. J. Biol. Macromol.*, 2012, **51**, 1116–1120 CrossRef CAS PubMed .
104. A. Salanti, L. Zoia, M. Orlandi, F. Zanini and G. Elegir, *J. Agric. Food Chem.*, 2010, **58**, 10049–10055 CrossRef CAS PubMed .
105. H. Sadeghifar and D. S. Argyropoulos, *ACS Sustainable Chem. Eng.*, 2015, **3**, 349–356 CrossRef CAS .
106. Y. Meng, J. Lu, Y. Cheng, Q. Li and H. Wang, *Int. J. Biol. Macromol.*, 2019, **135**, 1006–1019 CrossRef CAS PubMed .
107. M. Li, X. Jiang, D. Wang, Z. Xu and M. Yang, *Colloids Surf., B*, 2019, **177**, 370–376 CrossRef CAS PubMed .
108. T. Jayaramudu, H.-U. Ko, H. C. Kim, J. W. Kim, E. S. Choi and J. Kim, *Composites, Part B*, 2019, **156**, 43–50 CrossRef CAS .
109. Q. Yu, A. Bahi and F. Ko, *Macromol. Mater. Eng.*, 2015, **300**, 1023–1032 CrossRef CAS .
110. L. Bai, L. G. Greca, W. Xiang, J. Lehtonen, S. Huan, R. W. N. Nugroho, B. L. Tardy and O. J. Rojas, *Langmuir*, 2019, **35**, 571–588 CrossRef CAS PubMed .
111. L. Jing, X. Wang, H. Liu, Y. Lu, J. Bian, J. Sun and D. Huang, *ACS Appl. Mater. Interfaces*, 2018, **10**, 18551–18559 CrossRef CAS PubMed .

112. M. Oliviero, L. Verdolotti, E. Di Maio, M. Aurilia and S. Iannace, *J. Agric. Food Chem.*, 2011, **59**, 10062–10070 CrossRef CAS PubMed.
113. M. Oliviero, R. Rizvi, L. Verdolotti, S. Iannace, H. E. Naguib, E. Di Maio, H. C. Neitzert and G. Landi, *Adv. Funct. Mater.*, 2017, **27**, 1605142 CrossRef.
114. J. G. Lee, Y. Guo, J. A. Belgodere, A. Al Harraq, A. A. Hymel, A. J. Pete, K. T. Valsaraj, M. G. Benton, M. G. Miller, J. P. Jung and B. Bharti, *ACS Sustainable Chem. Eng.*, 2021, **9**, 1781–1789 CrossRef CAS.
115. A. A. Vaidya, C. Collet, M. Gaugler and G. Lloyd-Jones, *Mater. Today Commun.*, 2019, **19**, 286–296 CrossRef CAS.
116. S. L. Hilburg, A. N. Elder, H. Chung, R. L. Ferebee, M. R. Bockstaller and N. R. Washburn, *Polymer*, 2014, **55**, 995–1003 CrossRef CAS.
117. Y. Zhang, B. Yuan, Y. Zhang, Q. Cao, C. Yang, Y. Li and J. Zhou, *Chem. Eng. J.*, 2020, **400**, 125984 CrossRef CAS.
118. J. Yu, J. Wang, C. Wang, Y. Liu, Y. Xu, C. Tang and F. Chu, *Macromol. Rapid Commun.*, 2015, **36**, 398–404 CrossRef CAS PubMed.
119. J. Wang, L. Tian, B. Luo, S. Ramakrishna, D. Kai, X. J. Loh, I. H. Yang, G. R. Deen and X. Mo, *Colloids Surf., B*, 2018, **169**, 356–365 CrossRef CAS PubMed.
120. S. Jiang, D. Kai, Q. Q. Dou and X. J. Loh, *J. Mater. Chem. B*, 2015, **3**, 6897–6904 RSC.
121. Z. Liu, X. Lu, J. Xie, B. Feng and Q. Han, *Sep. Purif. Technol.*, 2019, **210**, 355–363 CrossRef CAS.
122. K. Guo, B. Gao, W. Wang, Q. Yue and X. Xu, *Chemosphere*, 2019, **215**, 214–226 CrossRef CAS PubMed.
123. Y. Qian, Q. Zhang, X. Qiu and S. Zhu, *Green Chem.*, 2014, **16**, 4963–4968 RSC.
124. D. Kai, S. Jiang, Z. W. Low and X. J. Loh, *J. Mater. Chem. B*, 2015, **3**, 6194–6204 RSC.
125. D. Kai, Z. W. Low, S. S. Liow, A. Abdul Karim, H. Ye, G. Jin, K. Li and X. J. Loh, *ACS Sustainable Chem. Eng.*, 2015, **3**, 2160–2169 CrossRef CAS.
126. R. Verduzco, X. Li, S. L. Pesek and G. E. Stein, *Chem. Soc. Rev.*, 2015, **44**, 2405–2420 RSC.
127. H.-i. Lee, J. Pietrasik, S. S. Sheiko and K. Matyjaszewski, *Prog. Polym. Sci.*, 2010, **35**, 24–44 CrossRef CAS.
128. C. Feng, Y. Li, D. Yang, J. Hu, X. Zhang and X. Huang, *Chem. Soc. Rev.*, 2011, **40**, 1282–1295 RSC.
129. H. Liu and H. Chung, *J. Polym. Sci., Part A: Polym. Chem.*, 2017, **55**, 3515–3528 CrossRef CAS.
130. W. Ren, X. Pan, G. Wang, W. Cheng and Y. Liu, *Green Chem.*, 2016, **18**, 5008–5014 RSC.
131. S. Y. Park, J.-Y. Kim, H. J. Youn and J. W. Choi, *Int. J. Biol. Macromol.*, 2019, **138**, 1029–1034 CrossRef CAS PubMed.

132. Y.-L. Chung, J. V. Olsson, R. J. Li, C. W. Frank, R. M. Waymouth, S. L. Billington and E. S. Sattely, *ACS Sustainable Chem. Eng.*, 2013, **1**, 1231–1238 CrossRef CAS .
133. D. Kai, W. Ren, L. Tian, P. L. Chee, Y. Liu, S. Ramakrishna and X. J. Loh, *ACS Sustainable Chem. Eng.*, 2016, **4**, 5268–5276 CrossRef CAS .
134. D. Kai, H. M. Chong, L. P. Chow, L. Jiang, Q. Lin, K. Zhang, H. Zhang, Z. Zhang and X. J. Loh, *Compos. Sci. Technol.*, 2018, **158**, 26–33 CrossRef CAS .
135. S. Laurichesse and L. Avérous, *Polymer*, 2013, **54**, 3882–3890 CrossRef CAS .
136. W. De Oliveira and W. G. Glasser, *J. Appl. Polym. Sci.*, 1994, **51**, 563–571 CrossRef CAS .
137. W. de Oliveira and W. G. Glasser, *Macromolecules*, 1994, **27**, 5–11 CrossRef CAS .
138. R. A. Pérez-Camargo, G. Saenz, S. Laurichesse, M. T. Casas, J. Puiggalí, L. Avérous and A. J. Müller, *J. Polym. Sci., Part B: Polym. Phys.*, 2015, **53**, 1736–1750 CrossRef .
139. M. Abdollahi, R. Bairami Habashi and M. Mohsenpour, *Ind. Crops Prod.*, 2019, **130**, 547–557 CrossRef CAS .
140. J. Tian, Y. Yang and J. Song, *Int. J. Biol. Macromol.*, 2019, **141**, 919–926 CrossRef CAS PubMed .
141. D. Kai, K. Zhang, S. S. Liow and X. J. Loh, *ACS Appl. Bio Mater.*, 2019, **2**, 127–134 CrossRef CAS .
142. B. V. K. J. Schmidt, V. Molinari, D. Esposito, K. Tauer and M. Antonietti, *Polymer*, 2017, **112**, 418–426 CrossRef CAS .
143. D. Mahata, M. Jana, A. Jana, A. Mukherjee, N. Mondal, T. Saha, S. Sen, G. B. Nando, C. K. Mukhopadhyay, R. Chakraborty and S. M. Mandal, *Sci. Rep.*, 2017, **7**, 46412 CrossRef CAS PubMed .
144. C. Gupta and N. R. Washburn, *Langmuir*, 2014, **30**, 9303–9312 CrossRef CAS PubMed .
145. Y. Sun, L. Yang, X. Lu and C. He, *J. Mater. Chem. A*, 2015, **3**, 3699–3709 RSC .
146. D. Kai, K. Zhang, L. Jiang, H. Z. Wong, Z. Li, Z. Zhang and X. J. Loh, *ACS Sustainable Chem. Eng.*, 2017, **5**, 6016–6025 CrossRef CAS .
147. T. Lorson, M. M. Lübtow, E. Wegener, M. S. Haider, S. Borova, D. Nahm, R. Jordan, M. Sokolski-Papkov, A. V. Kabanov and R. Luxenhofer, *Biomaterials*, 2018, **178**, 204–280 CrossRef CAS PubMed .
148. Y. Miura, *J. Mater. Chem. B*, 2020, **8**, 2010–2019 RSC .
149. Y. Sun, Z. Ma, X. Xu, X. Liu, L. Liu, G. Huang, L. Liu, H. Wang and P. Song, *ACS Sustainable Chem. Eng.*, 2020, **8**, 2267–2276 CrossRef CAS .
150. J. Wang, K. Yao, A. L. Korich, S. Li, S. Ma, H. J. Ploehn, P. M. Iovine, C. Wang, F. Chu and C. Tang, *J. Polym. Sci., Part A: Polym. Chem.*, 2011, **49**, 3728–3738 CrossRef CAS .

151. Y. Xu, L. Yuan, Z. Wang, P. A. Wilbon, C. Wang, F. Chu and C. Tang, *Green Chem.*, 2016, **18**, 4974–4981 RSC .

152. K. S. Silmore, C. Gupta and N. R. Washburn, *J. Colloid Interface Sci.*, 2016, **466**, 91–100 CrossRef CAS PubMed .

153. J. O. Akindoyo, M. D. H. Beg, S. Ghazali, M. R. Islam, N. Jeyaratnam and A. R. Yuvaraj, *RSC Adv.*, 2016, **6**, 114453–114482 RSC .

154. V. P. Saraf and W. G. Glasser, *J. Appl. Polym. Sci.*, 1984, **29**, 1831–1841 CrossRef CAS .

155. V. P. Saraf, W. G. Glasser, G. L. Wilkes and J. E. McGrath, *J. Appl. Polym. Sci.*, 1985, **30**, 2207–2224 CrossRef CAS .

156. T. Hatakeyama, Y. Asano and H. Hatakeyama, *Macromol. Symp.*, 2003, **197**, 171–180 CrossRef CAS .

157. T. Hatakeyama, Y. Izuta, S. Hirose and H. Hatakeyama, *Polymer*, 2002, **43**, 1177–1182 CrossRef CAS .

158. H. Chung and N. R. Washburn, *ACS Appl. Mater. Interfaces*, 2012, **4**, 2840–2846 CrossRef CAS PubMed .

159. Y. Han, L. Yuan, G. Li, L. Huang, T. Qin, F. Chu and C. Tang, *Polymer*, 2016, **83**, 92–100 CrossRef CAS .

160. C. Wang and R. A. Venditti, *ACS Sustainable Chem. Eng.*, 2015, **3**, 1839–1845 CrossRef CAS .

161. A. L. Korich, A. B. Fleming, A. R. Walker, J. Wang, C. Tang and P. M. Iovine, *Polymer*, 2012, **53**, 87–93 CrossRef CAS .

162. E. Zong, G. Huang, X. Liu, W. Lei, S. Jiang, Z. Ma, J. Wang and P. Song, *J. Mater. Chem. A*, 2018, **6**, 9971–9983 RSC .

163. H. Liu and H. Chung, *Macromolecules*, 2016, **49**, 7246–7256 CrossRef CAS .

164. M. S. Karunarathna, M. K. Lauer, T. Thiounn, R. C. Smith and A. G. Tennyson, *J. Mater. Chem. A*, 2019, **7**, 15683–15690 RSC .

165. M. S. Karunarathna, A. G. Tennyson and R. C. Smith, *J. Mater. Chem. A*, 2020, **8**, 548–553 RSC .

166. M. Jawerth, M. Johansson, S. Lundmark, C. Gioia and M. Lawoko, *ACS Sustainable Chem. Eng.*, 2017, **5**, 10918–10925 CrossRef CAS .

167. I. Ribca, M. E. Jawerth, C. J. Brett, M. Lawoko, M. Schwartzkopf, A. Chumakov, S. V. Roth and M. Johansson, *ACS Sustainable Chem. Eng.*, 2021, **9**, 1692–1702 CrossRef CAS .

168. M. Chauhan, M. Gupta, B. Singh, A. K. Singh and V. K. Gupta, *Eur. Polym. J.*, 2014, **52**, 32–43 CrossRef CAS .

169. M. Zieglowski, S. Trosien, J. Rohrer, S. Mehlhase, S. Weber, K. Bartels, G. Siegert, T. Trellenkamp, K. Albe and M. Biesalski, *Front. Chem.*, 2019, **7**, 562 CrossRef CAS PubMed .

170. S. Gómez-Fernández, L. Ugarte, T. Calvo-Correas, C. Peña-Rodríguez, M. A. Corcuera and A. Eceiza, *Ind. Crops Prod.*, 2017, **100**, 51–64 CrossRef.

171. T. Saito, J. H. Perkins, D. C. Jackson, N. E. Trammel, M. A. Hunt and A. K. Naskar, *RSC Adv.*, 2013, **3**, 21832–21840 RSC.

172. X. Bao, Y. Yu, Q. Wang, P. Wang and J. Yuan, *ACS Sustainable Chem. Eng.*, 2019, **7**, 12973–12980 CrossRef CAS.

173. L. Liu, C. He, M. Xiao, Z. An and S. Lv, *Appl. Catal., A*, 2020, **597**, 117541 CrossRef CAS.

174. H. Takeshima, K. Satoh and M. Kamigaito, *Macromolecules*, 2017, **50**, 4206–4216 CrossRef CAS.

175. A. S. Amarasekara, B. Wiredu and A. Razzaq, *Green Chem.*, 2012, **14**, 2395–2397 RSC.

176. A. S. Jaufurally, A. R. S. Teixeira, L. Hollande, F. Allais and P.-H. Ducrot, *ChemistrySelect*, 2016, **1**, 5165–5171 CrossRef CAS.

177. H. Liu, B. Lepoittevin, C. Roddier, V. Guerineau, L. Bech, J.-M. Herry, M.-N. Bellon-Fontaine and P. Roger, *Polymer*, 2011, **52**, 1908–1916 CrossRef CAS.

178. A. L. Holmberg, J. F. Stanzione, R. P. Wool and T. H. Epps III, *ACS Sustainable Chem. Eng.*, 2014, **2**, 569–573 CrossRef CAS.

179. S. Wang, A. W. Bassett, G. V. Wieber, J. F. Stanzione and T. H. Epps III, *ACS Macro Lett.*, 2017, **6**, 802–807 CrossRef CAS.

180. A. L. Holmberg, N. A. Nguyen, M. G. Karavolias, K. H. Reno, R. P. Wool and T. H. Epps III, *Macromolecules*, 2016, **49**, 1286–1295 CrossRef CAS.

181. J. Zhou, H. Zhang, J. Deng and Y. Wu, *Macromol. Chem. Phys.*, 2016, **217**, 2402–2408 CrossRef CAS.

182. S. Wang, L. Shuai, B. Saha, D. G. Vlachos and T. H. Epps III, *ACS Cent. Sci.*, 2018, **4**, 701–708 CrossRef CAS PubMed.

183. W. Qu, Y. Huang, Y. Luo, S. Kalluru, E. Cochran, M. Forrester and X. Bai, *ACS Sustainable Chem. Eng.*, 2019, **7**, 9050–9060 CrossRef CAS.

184. R. Kakuchi, S. Yoshida, T. Sasaki, S. Kanoh and K. Maeda, *Polym. Chem.*, 2018, **9**, 2109–2115 RSC.

185. Y. Terao, S. Sugihara, K. Satoh and M. Kamigaito, *Eur. Polym. J.*, 2019, **120**, 109225 CrossRef.

186. A. L. Flourat, J. Combes, C. Bailly-Maitre-Grand, K. Magnien, A. Haudrechy, J.-H. Renault and F. Allais, *ChemSusChem*, 2021, **14**, 118–129 CrossRef CAS PubMed.

187. Y. Terao, K. Satoh and M. Kamigaito, *Biomacromolecules*, 2019, **20**, 192–203 CrossRef CAS PubMed.

188. H. Takeshima, K. Satoh and M. Kamigaito, *ACS Sustainable Chem. Eng.*, 2018, **6**, 13681–13686 CrossRef CAS.

189. L. Mialon, A. G. Pemba and S. A. Miller, *Green Chem.*, 2010, **12**, 1704–1706 RSC.

190. A. G. Pemba, M. Rostagno, T. A. Lee and S. A. Miller, *Polym. Chem.*, 2014, **5**, 3214–3221 RSC.

191. S. V. Mankar, M. N. Garcia Gonzalez, N. Warlin, N. G. Valsange, N. Rehnberg, S. Lundmark, P. Jannasch and B. Zhang, *ACS Sustainable Chem. Eng.*, 2019, **7**, 19090–19103 CrossRef CAS.

192. Y. Peng, K. H. Nicastro, T. H. Epps III and C. Wu, *Food Chem.*, 2021, **338**, 127656 CrossRef CAS PubMed.

193. Y. Peng, K. H. Nicastro, T. H. Epps III and C. Wu, *J. Agric. Food Chem.*, 2018, **66**, 11775–11783 CrossRef CAS PubMed.

194. S. F. Koelewijn, C. Cooreman, T. Renders, C. Andecochea Saiz, S. Van den Bosch, W. Schutyser, W. De Leger, M. Smet, P. Van Puyvelde, H. Witters, B. Van der Bruggen and B. F. Sels, *Green Chem.*, 2018, **20**, 1050–1058 RSC.

195. S.-F. Koelewijn, D. Ruijten, L. Trullemans, T. Renders, P. Van Puyvelde, H. Witters and B. F. Sels, *Green Chem.*, 2019, **21**, 6622–6633 RSC.

196. G. Chandra, E. J. Nesakumar, V. R. G. Bhotla, S. G. Shetty, J. Mahood, R. R. Gallucci, J. H. Kamps and M. S. Kumar, *US Pat*, 9120893B1, 2015 Search PubMed.

197. K. H. Nicastro, C. J. Kloxin and T. H. Epps III, *ACS Sustainable Chem. Eng.*, 2018, **6**, 14812–14819 CrossRef CAS.

198. J. S. Mahajan, R. M. O'Dea, J. B. Norris, L. T. J. Korley and T. H. Epps III, *ACS Sustainable Chem. Eng.*, 2020, **8**, 15072–15096 CrossRef CAS.

199. M. Janvier, P.-H. Ducrot and F. Allais, *ACS Sustainable Chem. Eng.*, 2017, **5**, 8648–8656 CrossRef CAS.

200. O. Kreye, H. Mutlu and M. A. R. Meier, *Green Chem.*, 2013, **15**, 1431–1455 RSC.

201. M. Schmitt and V. Strehmel, *Org. Process Res. Dev.*, 2020, **24**, 2521–2528 CrossRef CAS.

202. C. Wulf, M. Reckers, A. Perechodjuk and T. Werner, *ACS Sustainable Chem. Eng.*, 2020, **8**, 1651–1658 CrossRef CAS.

203. K. Błażek, H. Beneš, Z. Walterová, S. Abbrent, A. Eceiza, T. Calvo-Correas and J. Datta, *Polym. Chem.*, 2021, **12**, 1643–1652 RSC.

204. M. Bourguignon, J.-M. Thomassin, B. Grignard, C. Jerome and C. Detrembleur, *ACS Sustainable Chem. Eng.*, 2019, **7**, 12601–12610 CAS.

205. S. Hu, X. Chen and J. M. Torkelson, *ACS Sustainable Chem. Eng.*, 2019, **7**, 10025–10034 CrossRef CAS.

206. M. Thébault, A. Pizzi, S. Dumarçay, P. Gerardin, E. Fredon and L. Delmotte, *Ind. Crops Prod.*, 2014, **59**, 329–336 CrossRef .

207. M. Thébault, A. Pizzi, H. A. Essawy, A. Barhoum and G. Van Assche, *Eur. Polym. J.*, 2015, **67**, 513–526 CrossRef .

208. A. Salanti, L. Zoia, M. Mauri and M. Orlandi, *RSC Adv.*, 2017, **7**, 25054–25065 RSC .

209. H. Chen, P. Chauhan and N. Yan, *Green Chem.*, 2020, **22**, 6874–6888 RSC .

210. I. Kühnel, B. Saake and R. Lehnen, *Macromol. Chem. Phys.*, 2018, **219**, 1700613 CrossRef .

211. D. V. Palaskar, A. Boyer, E. Cloutet, C. Alfos and H. Cramail, *Biomacromolecules*, 2010, **11**, 1202–1211 CrossRef CAS PubMed .

212. M. Fache, E. Darroman, V. Besse, R. Auvergne, S. Caillol and B. Boutevin, *Green Chem.*, 2014, **16**, 1987–1998 RSC .

213. R. Ménard, S. Caillol and F. Allais, *ACS Sustainable Chem. Eng.*, 2017, **5**, 1446–1456 CrossRef .

214. Q. Chen, K. Gao, C. Peng, H. Xie, Z. K. Zhao and M. Bao, *Green Chem.*, 2015, **17**, 4546–4551 RSC .

215. M. Parit and Z. Jiang, *Int. J. Biol. Macromol.*, 2020, **165**, 3180–3197 CrossRef CAS PubMed .

216. M. Ghorbani, F. Liebner, H. W. G. van Herwijnen, L. Pfungen, M. Krahofer, E. Budjav and J. Konnerth, *BioResources*, 2016, **11**(3), 6727–6741 CrossRef CAS .

217. B. Li, Y. Wang, N. Mahmood, Z. Yuan, J. Schmidt and C. Xu, *Ind. Crops Prod.*, 2017, **97**, 409–416 CrossRef CAS .

218. A. E. Vithanage, E. Chowdhury, L. D. Alejo, P. C. Pomeroy, W. J. DeSisto, B. G. Frederick and W. M. Gramlich, *J. Appl. Polym. Sci.*, 2017, **134**, 44827 CrossRef .

219. L. Fang, J. Zhou, Y. Tao, Y. Wang, X. Chen, X. Chen, J. Hou, J. Sun and Q. Fang, *ACS Sustainable Chem. Eng.*, 2019, **7**, 4078–4086 CrossRef CAS .

220. J. Chen, H. Liu, W. Zhang, L. Lv and Z. Liu, *J. Appl. Polym. Sci.*, 2020, **137**, 48827 CrossRef CAS .

221. M. Dai, Y. Tao, L. Fang, C. Wang, J. Sun and Q. Fang, *ACS Sustainable Chem. Eng.*, 2020, **8**, 15013–15019 CrossRef CAS .

222. E. A. Baroncini, S. K. Yadav, G. R. Palmese and J. F. Stanzione III, *J. Appl. Polym. Sci.*, 2016, **133**, 44103 CrossRef .

223. T. Liu, C. Hao, S. Zhang, X. Yang, L. Wang, J. Han, Y. Li, J. Xin and J. Zhang, *Macromolecules*, 2018, **51**, 5577–5585 CrossRef CAS .

224. S. Ma, J. Wei, Z. Jia, T. Yu, W. Yuan, Q. Li, S. Wang, S. You, R. Liu and J. Zhu, *J. Mater. Chem. A*, 2019, **7**, 1233–1243 RSC .

225. B. Wang, S. Ma, Q. Li, H. Zhang, J. Liu, R. Wang, Z. Chen, X. Xu, S. Wang, N. Lu, Y. Liu, S. Yan and J. Zhu, *Green Chem.*, 2020, **22**, 1275–1290 RSC.

226. E. Savonnet, C. Le Coz, E. Grau, S. Grelier, B. Defoort and H. Cramail, *Front. Chem.*, 2019, **7**, 606 CrossRef CAS PubMed.

227. S. Wang, S. Ma, C. Xu, Y. Liu, J. Dai, Z. Wang, X. Liu, J. Chen, X. Shen, J. Wei and J. Zhu, *Macromolecules*, 2017, **50**, 1892–1901 CrossRef CAS.

228. A. Maiorana, A. F. Reano, R. Centore, M. Grimaldi, P. Balaguer, F. Allais and R. A. Gross, *Green Chem.*, 2016, **18**, 4961–4973 RSC.

229. R. Ménard, S. Caillol and F. Allais, *Ind. Crops Prod.*, 2017, **95**, 83–95 CrossRef.

230. L. Hollande, I. Do Marcolino, P. Balaguer, S. Domenek, R. A. Gross and F. Allais, *Front. Chem.*, 2019, **7**, 159 CrossRef PubMed.

231. L. Hollande and F. Allais, in *Green Polymer Chemistry: New Products, Processes, and Applications*, American Chemical Society, 2018, vol. 1310, ch. 15, pp. 221–251 Search PubMed.

232. M. Janvier, L. Hollande, A. S. Jaufurally, M. Pernes, R. Ménard, M. Grimaldi, J. Beaugrand, P. Balaguer, P.-H. Ducrot and F. Allais, *ChemSusChem*, 2017, **10**, 738–746 CrossRef CAS PubMed.

233. Y. Tao, J. Zhou, L. Fang, Y. Wang, X. Chen, X. Chen, J. Hou, J. Sun and Q. Fang, *ACS Sustainable Chem. Eng.*, 2019, **7**, 7304–7311 CrossRef CAS.

234. L. Granado, R. Tavernier, S. Henry, R. O. Auke, G. Foyer, G. David and S. Caillol, *ACS Sustainable Chem. Eng.*, 2019, **7**, 7209–7217 CrossRef CAS.

235. C. J. Kloxin and C. N. Bowman, *Chem. Soc. Rev.*, 2013, **42**, 7161–7173 RSC.

236. N. J. Van Zee and R. Nicolaÿ, *Prog. Polym. Sci.*, 2020, **104**, 101233 CrossRef CAS.

237. W. Denissen, J. M. Winne and F. E. Du Prez, *Chem. Sci.*, 2016, **7**, 30–38 RSC.

238. Q. Li, S. Ma, P. Li, B. Wang, H. Feng, N. Lu, S. Wang, Y. Liu, X. Xu and J. Zhu, *Macromolecules*, 2021, **54**, 1742–1753 CrossRef CAS.

239. K.-K. Tremblay-Parrado, C. Bordin, S. Nicholls, B. Heinrich, B. Donnio and L. Avérous, *Macromolecules*, 2020, **53**, 5869–5880 CrossRef CAS.

240. D. Montarnal, M. Capelot, F. Tournilhac and L. Leibler, *Science*, 2011, **334**, 965 CrossRef CAS PubMed.

241. L. Yue, V. S. Bonab, D. Yuan, A. Patel, V. Karimkhani and I. Manas-Zloczower, *Global Challenges*, 2019, **3**, 1800076 CrossRef PubMed.

242. M. Röttger, T. Domenech, R. van der Weegen, A. Breuillac, R. Nicolaÿ and L. Leibler, *Science*, 2017, **356**, 62 CrossRef PubMed.

243. J. J. Lessard, G. M. Scheutz, S. H. Sung, K. A. Lantz, T. H. Epps III and B. S. Sumerlin, *J. Am. Chem. Soc.*, 2020, **142**, 283–289 CrossRef CAS PubMed .

244. J. A. Wilson, S. A. Hopkins, P. M. Wright and A. P. Dove, *ACS Macro Lett.*, 2016, **5**, 346–350 CrossRef CAS .

245. C. Hao, T. Liu, S. Zhang, L. Brown, R. Li, J. Xin, T. Zhong, L. Jiang and J. Zhang, *ChemSusChem*, 2019, **12**, 1049–1058 CrossRef CAS PubMed .

246. S. Zhang, T. Liu, C. Hao, L. Wang, J. Han, H. Liu and J. Zhang, *Green Chem.*, 2018, **20**, 2995–3000 RSC .

247. T. Liu, C. Hao, L. Wang, Y. Li, W. Liu, J. Xin and J. Zhang, *Macromolecules*, 2017, **50**, 8588–8597 CrossRef CAS .

248. H. Geng, Y. Wang, Q. Yu, S. Gu, Y. Zhou, W. Xu, X. Zhang and D. Ye, *ACS Sustainable Chem. Eng.*, 2018, **6**, 15463–15470 CrossRef CAS .

249. Y. Tao, L. Fang, J. Zhou, C. Wang, J. Sun and Q. Fang, *ACS Appl. Polym. Mater.*, 2020, **2**, 295–303 CrossRef CAS .

250. S. Wang, S. Ma, Q. Li, W. Yuan, B. Wang and J. Zhu, *Macromolecules*, 2018, **51**, 8001–8012 CrossRef CAS .

251. Z. Zhou, X. Su, J. Liu and R. Liu, *ACS Appl. Polym. Mater.*, 2020, **2**, 5716–5725 CrossRef CAS .

252. Q. Yu, X. Peng, Y. Wang, H. Geng, A. Xu, X. Zhang, W. Xu and D. Ye, *Eur. Polym. J.*, 2019, **117**, 55–63 CrossRef CAS .

253. C. J. Van Wyngaard, J. H. C. Pretorius and L. Pretorius, Theory of the triple constraint – A conceptual review, in *Proc. IEEE International Conference on Industrial Engineering and Engineering management (IEEM)*, Hong Kong, 2012, pp. 1991–1997 Search PubMed .

254. A. Guss, *Metabolic engineering for lignin conversion*, Oak Ridge National Laboratory, Oak Ridge, Tennesee, USA, 2019. https://www.energy.gov/sites/prod/files/2019/04/f61/Metabolic%20engineering%20for%20lignin%20conversion_NL0026701.pdf Search PubMed .

255. D. Salvachúa and G. T. Beckham, *Biological Lignin Valorization*, National Renewable Energy Laboratory, Golden, CO, USA, 2019. https://www.energy.gov/sites/prod/files/2019/04/f61/Biological%20Lignin%20Valorization%20%E2%80%93%20NREL_NL0026678.pdf Search PubMed .

256. C. C. Xu, L. Dessbesell, Y. Zhang and Z. Yuan, *Biofuels, Bioprod. Biorefin.*, 2021, **15**, 32–36 CrossRef CAS .

257. I. Graça, R. T. Woodward, M. Kennema and R. Rinaldi, *ACS Sustainable Chem. Eng.*, 2018, **6**, 13408–13419 CrossRef .

258. T. D. Ngo, A. Kashani, G. Imbalzano, K. T. Q. Nguyen and D. Hui, *Composites, Part B*, 2018, **143**, 172–196 CrossRef CAS .

259. R. Ding, Y. Du, R. B. Goncalves, L. F. Francis and T. M. Reineke, *Polym. Chem.*, 2019, **10**, 1067–1077 RSC .

260. Q. Shi, K. Yu, X. Kuang, X. Mu, C. K. Dunn, M. L. Dunn, T. Wang and H. J. Qi, *Mater. Horiz.*, 2017, **4**, 598–607 RSC .

Footnote

† These authors contributed equally to this work.